Identification of Vibration Signature for Grinding Process

Submitted By

Mostafa Rifat Anwar - 200012117

Khan Md Nafi - 200012152

Supervised By

Professor Dr. Md. Anayet Ullah Patwari

A Thesis submitted in partial fulfillment of the requirement for the degree of Bachelor of Science in Industrial and Production Engineering

Department of Mechanical and Production Engineering (MPE)

Islamic University of Technology (IUT)

October, 2025

Candidate's Declaration

This is to certify that the work presented in this thesis, titled "Identification of Vibration Signature for Grinding Process", is the outcome of the investigation and research carried out by us under the supervision of Dr. Md. Anayet Ullah Patwari, Professor, Department of Mechanical and Production Engineering, Islamic University of Technology.

It is also declared that neither this thesis nor any part of it has been submitted elsewhere for the award of any degree or diploma.

Mostafa Rifat Anwar
Student No: 200012117

Khan Md Nafi
Student No: 200012152

Recommendation of the Thesis Supervisor

The thesis titled "Identification of Vibration Signature for Grinding Process" submitted by Mostafa Rifat Anwar, Student No: 200012117, Khan Md Nafi, Student No: 200012152 has been accepted as satisfactory in partial fulfillment of the requirements for the degree of BSc. in Industrial and Production Engineering **on October, 2025.**

1. -------------------------------------
   Dr. Md. Anayet Ullah Patwari (Supervisor)
   Professor
   MPE Dept., IUT, Board Bazar, Gazipur-1704, Bangladesh.

CO-PO Mapping of ME 4800 -Theis and Project

COs	Course Outcomes (CO) Statement	(PO)	Addressed by	
CO1	Discover and Locate research problems and illustrate them via figures/tables or projections/ideas through field visit and literature review and determine/Setting aim and objectives of the project/work/research in specific, measurable, achievable, realistic and timeframe manner.	**PO2 Problem analysis**	Thesis Book	√
			Performance by research	√
			Presentation and soft skill	√
CO2	Design research solutions of the problems towards achieving the objectives and its application. Design systems, components or processes that meets related needs in the field of mechanical engineering	**PO3 Design/development of solutions**	Thesis Book	√
			Performance by research	√
			Presentation and soft skill	√
CO3	Review, debate, compare and contrast the relevant literature contents. Relevance of this research/study. Methods, tools, and techniques used by past researchers and justification of use of them in this work.	**PO4 Investigation**	Thesis Book	√
			Performance by research	√
			Presentation and soft skill	√
CO4	Analyse data and exhibit results using tables, diagrams, graphs with their interpretation. Investigate the designed solutions to solve the problems through case study/survey study/experimentation/simulation using modern tools and techniques.	**PO5 Modern tool usage**	Thesis Book	√
			Performance by research	√
			Presentation and soft skill	√
CO5	Apply moral values and research/professional ethics throughout the work, and justify genuine referencing on sources, and demonstration of own contribution.	**PO8 Ethics**	Thesis Book	√
			Performance by research	√
			Presentation and soft skill	√
CO6	Perform own self and manage group activities from the beginning to the end of the research/work as a quality work.	**PO9 Individual work and teamwork**	Thesis Book	√
			Performance by research	√
			Presentation and soft skill	√
CO7	Compile and arrange the work outputs, write the report/thesis, a sample journal paper, and present the work to wider audience using modern communication tools and techniques.	**PO10 Communication**	Thesis Book	√
			Performance by research	√
			Presentation and soft skill	√
CO8	Recognize the necessity of life-long learning in career development in dynamic real-world situations from the experience of completing this project.	**PO12 Life-long learning**	Thesis Book	√
			Performance by research	√
			Presentation and soft skill	√

Student Name /ID:

1. Mostafa Rifat Anwar / 200012117

2. Khan Md Nafi / 200012152

Signature of the Supervisor:

Name of the Supervisor:
Dr. Md. Anayet Ullah Patwari

K-P-A Mapping of ME 4800 -Theis and Project

COs	POs	Related Ks								Related Ps							Related As				
		K1	K2	K3	K4	K5	K6	K7	K8	P1	P2	P3	P4	P5	P6	P7	A1	A2	A3	A4	A5
CO1	PO2	√	√	√	√					√											
CO2	PO3					√				√	√	√				√	√	√	√		
CO3	PO4								√	√	√	√					√	√			
CO4	PO5						√			√				√							
CO5	PO8							√													
CO6	PO9																				
CO7	PO10																				
CO8	PO12																				

Student Name /ID:

1. Mostafa Rifat Anwar / 200012117

2. Khan Md Nafi / 200012152

Signature of the Supervisor:

Name of the Supervisor:
Dr. Md. Anayet Ullah Patwari

List of Sustainable Development Goals (SDGs) Addressed in this Project

SDG No.	Goals	Targets	Relevance to the Thesis (put √ if valid)	Remarks
1	No Poverty	1.1 Eradicate extreme poverty (people living on less than $1.25/day).		
		1.2 Reduce poverty in all its forms by at least half.		
		1.3 Implement nationally appropriate social protection systems.		
		1.4 Ensure equal rights to economic resources, services, property, inheritance, technology, and financial services.		
		1.5 Build resilience of the poor and reduce exposure to climate-related and other shocks.		
		1.a Mobilize resources to end poverty.		
		1.b Create pro-poor policy frameworks.		
2	Zero Hunger	2.1 End hunger and ensure access to safe, nutritious food year-round.		
		2.2 End all forms of malnutrition.		
		2.3 Double agricultural productivity and incomes of small-scale producers.		
		2.4 Ensure sustainable food production systems and resilient agricultural practices.		
		2.5 Maintain genetic diversity of seeds, plants, and animals.		
		2.a Increase investment in rural infrastructure, research, and technology.		
		2.b Correct and prevent trade restrictions/distortions in global food markets.		
		2.c Adopt measures to ensure proper functioning of food commodity markets.		
3	Good Health and Well-Being	3.1 Reduce global maternal mortality ratio.		
		3.2 End preventable deaths of newborns and under-5 children.		
		3.3 End epidemics of AIDS, tuberculosis, malaria, and neglected tropical diseases.		

		3.4 Reduce premature mortality from NCDs and promote mental health.		
		3.5 Strengthen prevention and treatment of substance abuse.		
		3.6 Halve global deaths/injuries from road traffic accidents.		
		3.7 Ensure universal access to sexual and reproductive healthcare.		
		3.8 Achieve universal health coverage.		
		3.9 Reduce deaths from hazardous chemicals, pollution, and contamination.		
		3.a Strengthen tobacco control (WHO FCTC).		
		3.b Support R&D of vaccines and medicines.		
		3.c Increase health financing and workforce.		
		3.d Strengthen capacity for early warning and risk management.		
4	Quality Education	4.1 Ensure all complete free, equitable, quality primary and secondary education.		
		4.2 Ensure access to quality early childhood development and pre-primary education.		
		4.3 Ensure equal access to affordable technical, vocational, and higher education.		
		4.4 Increase skills for employment and entrepreneurship.		
		4.5 Eliminate gender disparities in education.		
		4.6 Ensure literacy and numeracy for youth and adults.		
		4.7 Ensure learners acquire knowledge/skills for sustainable development.		
		4.a Build and upgrade education facilities that are inclusive and safe.		
		4.b Expand scholarships for developing countries.		
		4.c Increase supply of qualified teachers.		
5	Gender Equality	5.1 End all forms of discrimination against women and girls.		
		5.2 Eliminate violence against women and girls.		

		5.3 Eliminate harmful practices (child, early, forced marriage, FGM).		
		5.4 Recognize and value unpaid care and domestic work.		
		5.5 Ensure women's participation in leadership and decision-making.		
		5.6 Ensure universal access to reproductive health and rights.		
		5.a Undertake reforms to give women equal rights to resources.		
		5.b Enhance use of enabling technology to empower women.		
		5.c Adopt and strengthen policies and laws for gender equality.		
6	Clean Water and Sanitation	6.1 Achieve universal and equitable access to safe drinking water.		
		6.2 Achieve access to adequate sanitation and hygiene.		
		6.3 Improve water quality by reducing pollution.	√	Operations were performed without coolant as it is not environmentally friendly.
		6.4 Increase water-use efficiency and sustainable withdrawals.		
		6.5 Implement integrated water resources management.		
		6.6 Protect and restore water-related ecosystems.		
		6.a Expand international cooperation in water and sanitation.		
		6.b Support participation of local communities.		
7	Affordable and Clean Energy	7.1 Ensure universal access to affordable, reliable, modern energy services.		
		7.2 Increase substantially the share of renewable energy.		
		7.3 Double global rate of improvement in energy efficiency.		
		7.a Enhance international cooperation on clean energy research/technology.		
		7.b Expand infrastructure and upgrade technology for sustainable energy.		
8	Decent Work and Economic Growth	8.1 Sustain per capita economic growth.		
		8.2 Achieve higher levels of productivity through diversification, tech, and innovation.	√	Higher levels of productivity are achieved by

				introducing magnet and ultrasonic assisted grinding, which resulted better surface profile.
		8.3 Promote policies for decent job creation and entrepreneurship.		
		8.4 Improve resource efficiency in production and consumption.	√	The time and number of operations to obtain similar surface quality are minimized.
		8.5 Achieve full and productive employment for all.		
		8.6 Substantially reduce youth not in employment/education/training.		
		8.7 Eradicate forced labour, modern slavery, and child labour.		
		8.8 Protect labour rights and safe working environments.		
		8.9 Promote sustainable tourism.		
		8.a Increase aid for trade support.		
		8.b Develop a global youth employment strategy.		
9	Industry, Innovation, and Infrastructure	9.1 Develop quality, reliable, sustainable infrastructure.		
		9.2 Promote inclusive and sustainable industrialization.	√	Sustainable industrialization is supported by improving surface quality in grinding.
		9.3 Increase access of SMEs to financial services and integration into value chains.		
		9.4 Upgrade infrastructure for sustainability and resource efficiency.		
		9.5 Enhance scientific research and technology development.	√	Technology development is enhanced by proposing new methods of grinding.
		9.a Facilitate sustainable infrastructure in developing countries.		

		9.b Support domestic tech development and value addition.		
		9.c Increase access to ICT and internet.		
10	Reduced Inequalities	10.1 Achieve income growth of bottom 40%.		
		10.2 Empower and promote inclusion regardless of status.		
		10.3 Ensure equal opportunity and reduce inequalities of outcome.		
		10.4 Adopt policies for fiscal, wage, and social protection equality.		
		10.5 Improve regulation of global financial markets.		
		10.6 Ensure enhanced representation in global institutions.		
		10.7 Facilitate safe, regular, and responsible migration.		
		10.a Implement special treatment for developing countries.		
		10.b Encourage development assistance and investment in least developed areas.		
		10.c Reduce remittance costs.		
11	Sustainable Cities and Communities	11.1 Ensure access to adequate, safe, and affordable housing.		
		11.2 Provide sustainable transport systems.		
		11.3 Enhance inclusive urbanization and capacity for planning.		
		11.4 Protect cultural and natural heritage.		
		11.5 Reduce disaster impact and losses.		
		11.6 Reduce environmental impact of cities (air quality, waste).		
		11.7 Provide access to safe, inclusive green/public spaces.		
		11.a Support positive links between urban, peri-urban, rural.		
		11.b Increase disaster risk reduction strategies.		
		11.c Support least developed countries in sustainable building.		
12	Responsible Consumption and Production	12.1 Implement 10-Year Framework on sustainable consumption/production.		
		12.2 Achieve sustainable management and use of resources.	√	No unnecessary operation was performed, thus sustainable management and use of

				resources were achieved.
		12.3 Halve per capita global food waste.		
		12.4 Manage chemicals and waste sustainably.	√	The waste was discharged in a specific place.
		12.5 Substantially reduce waste generation.		
		12.6 Encourage companies to adopt sustainable practices.		
		12.7 Promote sustainable public procurement.		
		12.8 Ensure people have relevant information for sustainable development.		
		12.a Support developing countries' scientific and technological capacity.		
		12.b Develop tools to monitor sustainable tourism impacts.		
		12.c Rationalize inefficient fossil-fuel subsidies.		
13	Climate Action	13.1 Strengthen resilience and adaptive capacity to climate-related hazards.		
		13.2 Integrate climate measures into national policies.		
		13.3 Improve education and awareness on climate change.		
		13.a Implement UNFCCC commitments (mobilize $100 billion annually).		
		13.b Promote mechanisms for capacity-building in least developed countries.		
14	Life Below Water	14.1 Reduce marine pollution.		
		14.2 Sustainably manage and protect marine ecosystems.		
		14.3 Minimize and address ocean acidification.		
		14.4 Regulate harvesting and end overfishing.		
		14.5 Conserve at least 10% of coastal and marine areas.		
		14.6 Prohibit harmful fisheries subsidies.		
		14.7 Increase economic benefits from sustainable marine resources.		
		14.a Increase scientific knowledge and marine technology transfer.		
		14.b Provide access for small-scale artisanal fishers.		

		14.c Implement international law for oceans.		
15	Life on Land	15.1 Conserve terrestrial and freshwater ecosystems.		
		15.2 Promote sustainable management of forests.		
		15.3 Combat desertification and restore degraded land.		
		15.4 Ensure conservation of mountain ecosystems.		
		15.5 Take urgent action to reduce biodiversity loss.		
		15.6 Promote fair benefit-sharing from genetic resources.		
		15.7 End poaching and trafficking of protected species.		
		15.8 Prevent introduction of invasive alien species.		
		15.9 Integrate ecosystem values into policies/planning.		
		15.a Mobilize resources for biodiversity.		
		15.b Finance sustainable forest management.		
		15.c Support local communities for forest and wildlife.		
16	Peace, Justice and Strong Institutions	16.1 Reduce violence and related death rates.		
		16.2 End abuse, trafficking, and violence against children.		
		16.3 Promote rules of law and equal access to justice.		
		16.4 Reduce illicit financial/arms flows, organized crime.		
		16.5 Reduce corruption and bribery.		
		16.6 Develop effective, accountable institutions.		
		16.7 Ensure inclusive, participatory decision-making.		
		16.8 Broaden participation of developing countries in global governance.		
		16.9 Provide legal identity for all (including birth registration).		
		16.10 Ensure access to information and protect freedoms.		
		16.a Strengthen national institutions for prevention of violence.		

		16.b Promote/enforce non-discriminatory laws and policies.		
17	Partnerships for the Goals	17.1 Strengthen domestic resource mobilization.		
		17.2 Developed countries to implement ODA commitments.		
		17.3 Mobilize additional financial resources.		
		17.4 Assist developing countries with debt sustainability.		
		17.5 Invest in least developed countries.		
		17.6 Enhance access to science, technology, innovation.		
		17.7 Promote environmentally sound technologies.		
		17.8 Fully operationalize technology bank for LDCs.		
		17.9 Enhance international support for capacity-building.		
		17.10 Promote a universal, rules-based trading system (WTO).		
		17.11 Increase exports of developing countries.		
		17.12 Timely implementation of duty-free, quota-free market access.		
		17.13 Enhance global macroeconomic stability.		
		17.14 Enhance policy coherence for sustainable development.		
		17.15 Respect national policy space.		
		17.16 Enhance global partnerships.		
		17.17 Encourage multi-stakeholder partnerships.		
		17.18 Enhance data capacity of developing countries.		
		17.19 Support capacity-building for sustainable development indicators.		

Acknowledgment

In the name of Allah, the Most Gracious, the Most Merciful.

All praise and thanks are to Allah, the Almighty, by whose grace and blessings this work has been brought to completion. His infinite mercy has been our greatest strength throughout this journey. Without His mercy, blessings, and guidance, none of our efforts would have come to fruition.

We wish to express our deepest gratitude to our respected supervisor, Dr. Md. Anayet Ullah Patwari, Professor, Department of Mechanical and Production Engineering, Islamic University of Technology. His invaluable guidance, constant encouragement, and unwavering patience have been essential throughout every stage of this thesis. Without his supervision and guidance, we would not be able to come this far. We are truly honored to have the opportunity to work under his supervision.

We are also grateful to workshop instructor Mr. Rajaul Karim for his cooperation and technical assistance during the experimental work. His contributions have been critical to the success of our thesis.

No amount of gratitude can truly repay our parents. Their endless love, sacrifices, and prayers have carried us through the most difficult times. Their faith in our abilities and their constant support have been our greatest source of strength. Without their guidance and sacrifice from childhood until today, this milestone would not have been possible.

Finally, we humbly pray to Allah (SWT) to accept this humble effort from us, to forgive our shortcomings, and to allow this work to be of benefit in the pursuit of knowledge and service to humanity. We accept any shortcomings in this work as our own, and we attribute all the good in it to the grace of Allah. May He continue to guide us in all our future endeavors. Ameen.

Abstract

Grinding is one of the most important finishing operations in modern manufacturing. Despite its widespread use, the grinding process faces several challenges, including vibrations, chatter, thermal damage, and grinding wheel wear, all of which can reduce productivity. This thesis investigates the identification and analysis of vibration signatures in the grinding process to develop a framework for real-time condition monitoring. Experimental studies were conducted to evaluate the effects of Magnetic Field-Assisted Grinding (MFAG) and Ultrasonic Vibration-Assisted Grinding (UVAG) on surface roughness in cylindrical grinding of mild steel. The experiments involved a structured sequence of operations: conventional grinding to establish a baseline, followed by MFAG and UVAG under varying process parameters. In MFAG, a static magnetic field was applied at different distances from the workpiece. Results demonstrated a complex interaction, where the magnetic field reduced surface finish by 35.38% under specific conditions (3 mm magnet distance) compared to conventional grinding (33.7%), but also revealed 2 mm magnet distance at low depth of cut showing better surface finish. In UVAG, the application of ultrasonic vibrations proved highly effective but distinctly frequency-specific. A frequency of 40 kHz yielded the most significant improvement, achieving a 35.54% reduction in surface roughness. A quadratic mathematical model for the UVAG process was developed by utilizing a Central Composite Design (CCD) and Analysis of Variance (ANOVA). The model identified workpiece rotational speed (RPM) as the most influential parameter affecting surface roughness. Subsequent optimization through desirability function analysis determined the ideal parameter combination for minimizing surface roughness to be an ultrasonic frequency of 31.8 kHz, a depth of cut of 0.092, and a workpiece RPM of 336, predicting an optimal surface roughness (Ra) of 2.88 µm. The study concludes that vibration signature analysis, combined with advanced assistance techniques, offers a viable pathway for real-time grinding process monitoring and control, contributing to enhanced manufacturing precision and efficiency.

Summary

In modern manufacturing, many important products such as aircraft parts, vehicle parts, and electronic devices require very smooth surfaces. To achieve this, industries use a process called grinding. Although grinding is widely used, it faces several problems. The most common issues are unwanted vibrations, heat damage, and tool wear. Vibrations in the grinding machine can create a pattern on the part's surface, making it less smooth. Heat produced during the process can cause the material to burn, reducing its strength and durability. Over time, the grinding wheel also becomes worn out, which increases the risk of poor-quality surfaces. All these problems can lead to wasted time, higher costs, and rejected parts. This thesis explores new ways to make grinding more efficient. Two techniques were studied in addition to the traditional method: applying magnet and applying ultrasonic frequencies. The experiments were carried out on cylindrical steel workpieces. In magnet assisted grinding, a magnet was placed close to the workpiece. In ultrasonic assisted grinding, ultrasonic vibrations were applied to the workpiece. The results showed that magnet assisted grinding improved the surface finish slightly better than normal grinding. The ultrasonic method showed that at a specific frequency around 40 kHz, the surface was the smoothest. An equation for the ultrasonic method was developed, which can predict how smooth a surface will be based on several factors. This allows operators to select the best combination of settings before starting the grinding process, saving both time and resources. In conclusion, this study shows that using smart techniques such as magnetic fields and ultrasonic vibrations can improve the grinding process. This research is a step toward smarter, more efficient, and more sustainable manufacturing, which is important for producing high-quality products in industries.

Table of Contents

Abstract **15**

Chapter 1: Introduction **23**

1.1 Background and Context 23

1.2 Methodologies for Capturing and Analyzing Vibration Data 24

1.3 Research Objectives 27

1.4 Problem Statement 27

1.5 Thesis Structure 27

1.6 Thesis Methodology 28

1.7 Thesis Outcomes 29

Chapter 2: Literature Review **30**

2.1 The Significance of Vibration Monitoring in Grinding 31

2.2 Theoretical Background of Vibration Analysis 32

2.3. Applications of Vibration Signature Analysis in Grinding 34

2.4. Research Gaps in Vibration Monitoring 35

2.5. Recent Advancements and Future Trends 36

2.6 Conclusion 37

Chapter 3: Methodology 39

3.1 Introduction 39

3.2 Theoretical and Foundational Concepts 41

3.3 Materials and Experimental Equipment 42

3.4 Process Parameters 46

3.4 Experimental Sequence 48

3.5 Data Collection 48

3.7 Limitations and Mitigations 49

3.8 Summary 50

Chapter 4: Results and Discussions 51

4.1 Introduction 51

4.2 Conventional Grinding 51

4.3 Magnetic Field Assisted Grinding 52

4.4 Ultrasonic Vibration Assisted Grinding 54

4.5 Mathematical Model Development Using Central Composite Design 59

4.6 Optimization by Desirability Analysis 65

4.7 Summary 67

Chapter 5: Conclusions and Future Recommendations 69

5.1 Introduction 69

5.2 Implications of the Study 71

5.3 Acknowledgment of Limitations 72

5.4 Future Recommendations 73

5.5 Concluding Remarks 74

References 75

List of Figures

Figure 1.1: Grinding operation (Source: Internet) 23
Figure 1.2: Kistler 9119AA2 dynamometer (Source: Internet) 25
Figure 1.3: Acceleration sensor (Souce: Internet) 25
Figure 1.4: Acoustic Emission Sensor (source: Internet) 26
Figure 1.5: FLIR E76 thermal camera (Source: Internet) 26
Figure 1.6: Flowchart of the thesis 28
Figure 2.1: Types of literature studied and reviewed 30
Figure 2.2: Chatter vibrations in grinding processes (Inasaki, 2001) 33
Figure 2.3: Active Damping System (Ahrens et al., 2014) 36
Figure 3.1: Flowchart of the research 40
Figure 3.2: Workpiece 42
Figure 3.3: Universal Cylindrical Grinding Machine 43
Figure 3.4: Magnet with holder setup 44
Figure 3.5: Magnet 44
Figure 3.6: UAV setup on grinding machine 45
Figure 3.7: Ultrasonic Assisted Vibration 45
Figure 3.8: Stand 45
Figure 3.9: Surface Roughness Tester 45
Figure 3.10: Measuring surface roughness 49
Figure 4.1: Workpiece surface before grinding 51
Figure 4.2: Workpiece surface after grinding 51
Figure 4.3: Workpiece surface after grinding with magnet 52
Figure 4.4: Variation of surface roughness at different magnet distances and depth of cut 53
Figure 4.5: Variations of surface roughness at different ultrasonic frequencies 55
Figure 4.6: Workpiece surfaces of grinding at different frequencies 56
Figure 4.7: Variation of surface roughness at different ultrasonic frequencies and depth of cuts 57
Figure 4.8: Predicted vs Actual surface roughness plot 63
Figure 4.9: Perturbation analysis plot 64
Figure 4.10: 3D Response surface plots of Ln(Ra) vs DOC vs UAV 64
Figure 4.11: 3D response surface plot of Ln(Ra) vs RPM vs UAV 65
Figure 4.12: Desirability optimization plots 66

List of Tables

Table 3.1: Grinding Machine Specification 43
Table 3.2: Surface Roughness Tester Machine Specification 46
Table 3. 3: Fixed Process Parameters 46
Table 3.4: Process Parameters for Initial Grinding Without Magnet, With Magnet, and With UAV 47
Table 3.5: Process Parameters for Magnet and Ultrasonic Assisted Grinding Under Varying Parameters 47
Table 3.6: Process Parameters for Grinding with UAV for Mathematical Model Development 47
Table 4.1: Surface Roughness in Conventional Grinding 51
Table 4.2: Surface Roughness in MFAG at Constant Magnet to Workpiece Distances and DOC 52
Table 4.3: Surface Roughness in MFAG at Different Magnet Distances and DOC 52
Table 4.4: Workpiece Surface Images in MFAG at Different Magnet Distances and DOC ... 54
Table 4.5: Surface Roughness in UVAG at Constant Feed 55
Table 4.6 Surface Roughness in UVAG at different frequencies and DOC 56
Table 4.7: Workpiece Surface Images in UVAG at different frequencies and DOC 58
Table 4.8: Coded Values for UAV, DOC and RPM 59
Table 4.9: Central Composite Design Matrix 60
Table 4.10: Sequential Model Sum of Squares 61
Table 4.11: Analysis of Variance Table (Partial Sum of Squares) 62
Table 4.12: Desirability Function Analysis 66

Nomenclatures and Symbols

Abbreviation	Meaning
ANOVA	Analysis of Variance
CCD	Central Composite Design
DOC	Depth of Cut
MFAG	Magnetic Field Assisted Grinding
RPM	Revolutions Per Minute
RSM	Response Surface Methodology
UAV	Ultrasonic Assisted Vibration
UVAG	Ultrasonic Vibration Assisted Grinding

List of symbols:

R_a - Arithmetic Average Surface Roughness

A - Ultrasonic Frequency

B - Depth of Cut

C - Workpiece RPM

Ln - Natural Logarithm

D - Overall Desirability

Chapter 1: Introduction

1.1 Background and Context

Grinding is a machining operation that removes material from the workpiece with an abrasive wheel, as shown in Figure 1.1. The grinding process holds a position of strategic importance in modern manufacturing, serving as a critical finishing operation for high-value components where precision is paramount. The ability to understand and control the complex dynamics of this process is fundamental to producing parts for demanding sectors such as aerospace, automotive, and medical technology. As a finishing procedure, grinding is indispensable for achieving precise final dimensions, adhering to tight geometric tolerances, and producing superior surface finishes that directly influence the functional performance and service life of a component.

Figure 1.1: Grinding operation (Source: Internet)

Defined as a precision machining process, grinding utilizes a rotating abrasive wheel to remove material from a workpiece. At the micro-scale, the material removal mechanism for ductile materials involves a sequence of physical interactions at the abrasive grain level, progressing through distinct stages of rubbing, ploughing, and cutting forces (Li et al., 2012). Its primary role is to refine parts that have undergone prior machining, ensuring they meet exacting standards for accuracy and surface integrity. However, the inherent physics of the process—characterized by intense friction, high temperatures, and complex tool-workpiece interactions—presents a set of formidable challenges that can compromise both quality and productivity. These challenges include:

Self-Excited Vibrations (Chatter): Grinding chatter is a regenerative, self-excited vibration that stands as one of the most significant limiting factors in process stability and productivity. This phenomenon arises from the dynamic interaction between the machine tool structure and the cutting process, causing a characteristic waviness to form on the surfaces of both the grinding wheel and the workpiece. The presence of chatter not only degrades the surface finish but also increases process forces, potentially damaging the machine and the component (Ahrens et al., 2014; Altintas & Weck, 2004).

Thermal Damage: The grinding process generates intense localized heat, which, if not properly managed, can inflict severe thermal damage on the workpiece surface. This damage manifests as grinding burns, which modify local hardness and can induce undesirable tensile residual stresses. Such metallurgical flaws can shorten the fatigue life of critically loaded components and, in severe cases, lead to the formation of microcracks and catastrophic failures (Malkin & Guo, 2007; Santa-aho et al., 2012).

Tool Wear and Degradation: The effectiveness of the grinding wheel diminishes over time due to progressive wear of the abrasive grains and the adhesion of workpiece material (chips) to the wheel surface. This degradation reduces the cutting efficiency of the wheel, leading to increased grinding forces, higher temperatures, and a marked deterioration in surface quality (Qiu et al., 2022).

Failure to effectively manage these phenomena has significant consequences, including production loss, high rates of part rejection, and the need for frequent and time-consuming dressing operations to restore the grinding wheel's condition. In severe cases, uncontrolled process dynamics can cause damage to both the machine tool and the workpiece, leading to costly downtime and repairs (Ahrens et al., 2014). This reality underscores the critical importance of robust process monitoring and control. Consequently, there is a compelling need to develop advanced, real-time monitoring techniques capable of detecting and diagnosing process anomalies before they compromise product quality.

1.2 Methodologies for Capturing and Analyzing Vibration Data

1.2.1 Context and Strategic Importance

The methodologies for monitoring vibrations in grinding have evolved significantly, moving from simple, post-process checks to sophisticated, real-time systems capable of in-process control. The effectiveness of any monitoring strategy is determined by the synergy between its components: the sensor technology used to capture physical phenomena and the analytical approach used to interpret the resulting data. The choice and integration of these methodologies are of paramount strategic importance, as they directly dictate the quality of actionable intelligence that can be derived from the process and ultimately determine the success of any control or optimization effort.

1.2.2 Data Capture and Sensor Technologies

A diverse array of sensors has been deployed to capture the dynamic and thermal signatures of the grinding process. The selection of a particular sensor depends on the specific process variable of interest, the required bandwidth and accuracy, and the harshness of the operating environment. Key technologies identified in the literature are:

1. **Piezoelectric Dynamometers:** Measure dynamic forces (normal and tangential) with high accuracy. Used for fundamental process analysis, force control, and chatter detection (e.g., Kistler 9257B, 9119AA2) (Ahrens et al., 2014; Wu et al., 2023) as shown in Figure 1.2.

Figure 1.2: Kistler 9119AA2 dynamometer (Source: Internet)

2. **Acceleration Sensors:** Measure the acceleration of machine or workpiece components. Primarily used to validate vibration measurements and study system dynamics (Ahrens et al., 2014), as shown in Figure 1.3.

Figure 1.3: Acceleration sensor (Souce: Internet)

3. **Acoustic Emission Sensors:** Detect high-frequency stress waves generated by material deformation and fracture. Used for process monitoring and validation of chatter detection algorithms (Ahrens et al., 2014), as shown in Figure 1.4.

Figure 1.4: Acoustic Emission Sensor (source: Internet)

4. Infrared Thermography: Non-contact measurement of temperature distribution in the grinding zone. Used to study thermal effects and validate thermo-mechanical models (e.g., FLIR E76) (Huang et al., 2025), as shown in Figure 1.5.

Figure 1.5: FLIR E76 thermal camera (Source: Internet)

5. Barkhausen Noise Sensors: Measure changes in micromagnetic properties to non-destructively assess surface integrity. Used to detect grinding burn by correlating signals to residual stress and hardness (e.g., 3MA-II, Rollscan) (Jedamski et al., 2020).

1.3 Research Objectives

This section outlines the primary aim and the specific, measurable objectives designed to systematically address the research problem defined above. The objectives form a structured pathway for developing a vibration-based diagnostic framework for real-time condition monitoring in grinding.

The primary aim of this research is to identify and analyze characteristic vibration signatures in the grinding process to serve as a diagnostic tool for real-time condition monitoring.

To achieve this primary aim, the following specific objectives have been established:

1) To investigate how magnetic field and ultrasonic frequency affect grinding process by measuring surface roughness.

2) To build a mathematical model on how different process parameters affect surface roughness in ultrasonic vibration assisted grinding.

3) To propose a new method of grinding using magnet and ultrasonic vibration.

The following section provides a roadmap for the structure of this thesis.

1.4 Problem Statement

Grinding creates vibrations and chatter during operation, which leads to poor surface finish and worsens overall product quality. An effective and efficient grinding process needs to be adapted to improve the quality of surface.

1.5 Thesis Structure

This section provides a clear and concise overview of the organization of the thesis, guiding the reader through the subsequent chapters. There are 5 chapters in the thesis. They are as follows:

Chapter 1: Introduction: Presents an overview of grinding, background of the thesis, causes of vibrations in grinding, states the research objectives and problem statement, and outlines the overall structure of the thesis.

Chapter 2: Literature Review: Presents a comprehensive review of existing research on grinding mechanics, process monitoring techniques, and vibration analysis in machining.

Chapter 3: Methodology: Describes the detailed experimental setup, data acquisition system, and the analytical techniques used to measure surface roughness.

Chapter 4: Results and Discussion: Presents the experimental findings, and discusses their correlation with specific grinding phenomena.

Chapter 5: Conclusion and Future Recommendations: Summarizes the key findings of the research, discusses their implications, and provides recommendations for future work in this area.

1.6 Thesis Methodology

The research was conducted in 5 steps. They are summarized as follows:

1) Conventional Grinding: Cylindrical workpieces were selected, and one was ground conventionally to obtain baseline surface roughness.

2) Magnet Assisted Grinding: Grinding operations were done by applying magnetic field first at a fixed distance and constant depth of cut to compare it with conventional grinding, then at varying distances and depth of cuts to study the parameters' effect on surface roughness.

3) Ultrasonic Assisted Grinding: Grinding operations were performed by applying ultrasonic vibrations first at different frequencies and constant depth of cut to test against conventional grinding, then at varying frequencies and depth of cuts to examine parameter effects.

4) Mathematical Model Development: In ultrasonic assisted grinding, experiments were conducted at different ultrasonic frequencies, depth of cuts, and workpiece RPM. The resulting surface roughness data were used to build a quadratic model using Central Composite Design (CCD), validated with ANOVA.

5) Optimization by Desirability Analysis: The developed model was optimized through desirability analysis to identify parameter values that minimize surface roughness.

Figure 1.6 shows the summarized flowchart of the overall thesis.

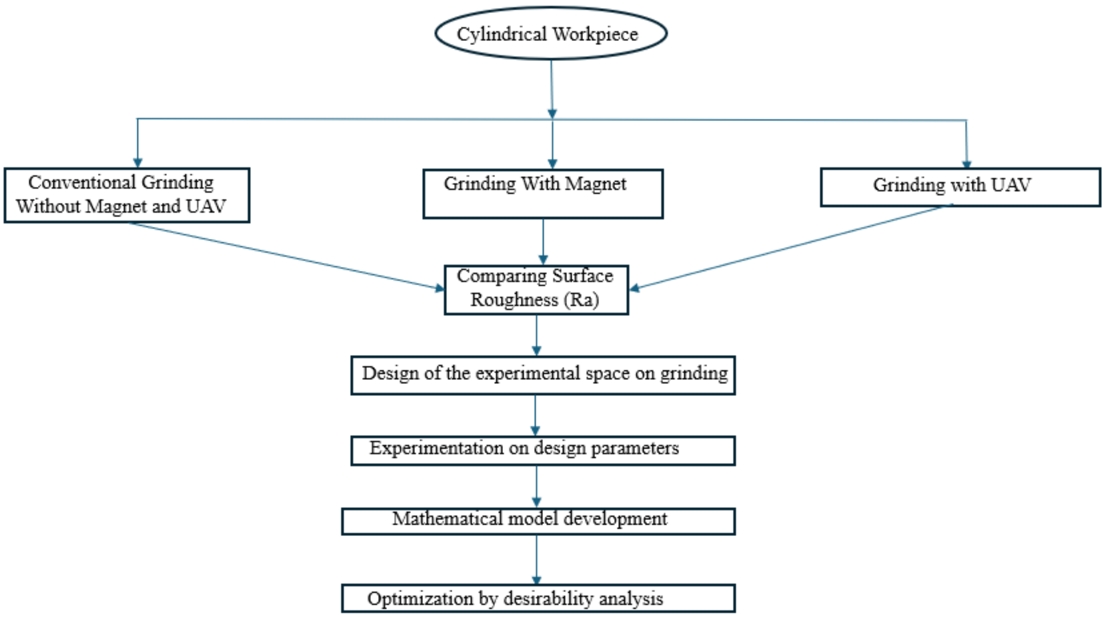

Figure 1.6: Flowchart of the thesis

1.7 Thesis Outcomes

The outcomes of the thesis are as follows:

1) Applying magnetic field and ultrasonic vibrations improved grinding process by reducing surface roughness more than the conventional one.

2) A mathematical model was developed in ultrasonic assisted grinding to predict surface roughness in different parameter combinations.

3) Innovative grinding processes by the application of magnetic field and ultrasonic vibrations are proposed.

Chapter 2: Literature Review

Precision grinding is a critical final-stage manufacturing process where surface integrity and dimensional accuracy are paramount. As a finishing operation, it is responsible for imparting the final geometric and functional characteristics to high-performance components. Unwanted vibrations, however, are a primary limiting factor to achieving optimal outcomes, manifesting as surface defects, accelerated tool wear, and reduced productivity. The analysis of vibration signatures thus represents a crucial frontier in the pursuit of more intelligent and reliable grinding operations. This chapter synthesizes the existing body of research on the monitoring, analysis, and interpretation of vibration signatures to control and optimize the grinding process. It reviews the strategic importance of vibration monitoring, the theoretical underpinnings of vibration analysis, the methodologies for data capture, and the practical applications of this knowledge, from active chatter suppression to real-time anomaly detection. By examining both the successes and persistent challenges in the field, this review charts the evolution from post-process inspection toward data-driven, in-process control.

Figure 2.1 illustrates the types of literature studied.

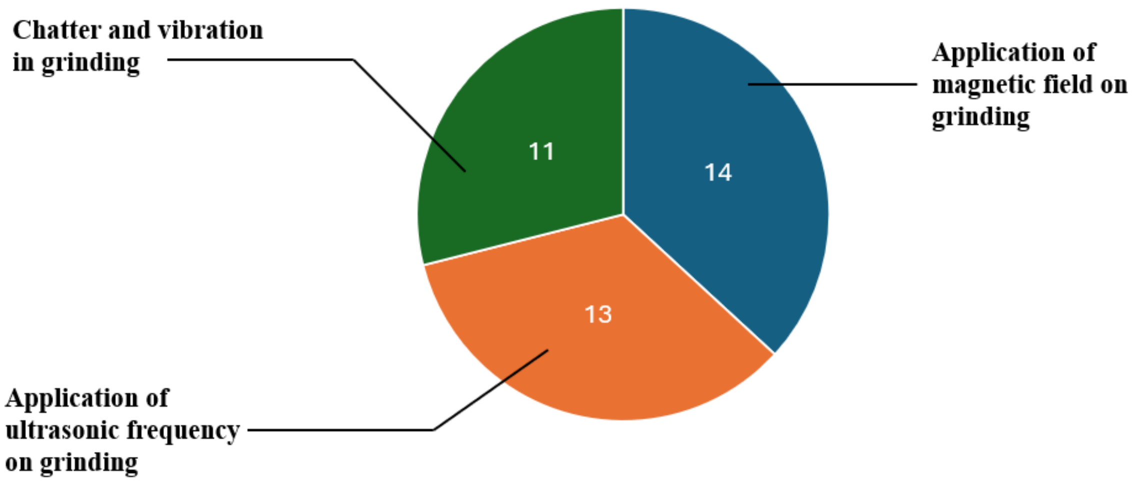

Figure 2.1: Types of literature studied and reviewed

2.1 The Significance of Vibration Monitoring in Grinding

2.1.1 Context and Strategic Importance

In the domain of high-precision manufacturing, the grinding process is the physical interface where the complex dynamics of the tool, workpiece, and machine converge. The vibrations arising from this interaction are not stochastic noise but rather a data-rich signal containing detailed information about the state of the process. Monitoring these vibrations is therefore not merely a diagnostic task but a strategic necessity for ensuring product quality, maximizing process efficiency, and preserving the longevity of critical manufacturing equipment. The ability to capture and interpret these dynamic signatures is fundamental to advancing grinding from a craft reliant on operator experience to a predictable, controllable, and optimized science.

2.1.2 The Role of Vibration in Process Outcomes

Vibrations, and the forces they represent, have a direct and measurable impact on nearly every critical outcome of the grinding process. Research has consistently demonstrated a strong correlation between vibration signatures and grinding force, which in turn governs the quality, efficiency, and health of the operation.

Product Quality: Uncontrolled vibrations are a primary cause of surface and subsurface defects. The regenerative instability known as chatter, for instance, leaves characteristic wave-like marks on the workpiece surface, compromising dimensional accuracy and surface integrity (Ahrens et al., 2014). The grinding force, intrinsically linked to vibration, is a key determinant of these outcomes.

Process Efficiency: Process stability is often limited by the onset of self-excited vibrations. To avoid chatter and other dynamic instabilities, operators are often forced to use conservative process parameters, such as lower material removal rates. This directly reduces productivity and increases cycle times, making vibration a significant bottleneck in high-volume production (Ahrens et al., 2014).

Tool and Machine Health: The forces associated with excessive vibration lead to accelerated wear of the grinding wheel, causing uneven wear patterns and waviness on the wheel surface. Over time, these uncontrolled dynamic loads can propagate through the machine structure, potentially damaging sensitive components such as spindles and guideways (Ahrens et al., 2014). This link between dynamic forces and wear is foundational to modern process monitoring.

2.1.3 Vibration Signatures as Diagnostic Tools

By analyzing vibration and its related process signals, it becomes possible to diagnose critical process anomalies in real-time, enabling a shift from reactive, post-process inspection to proactive, in-process control. Indirect measurement techniques have proven effective at detecting thermo-mechanical damage. Micromagnetic methods, particularly Barkhausen noise analysis, can identify grinding burn by measuring changes in magnetic properties that correlate with undesirable hardness reductions and the development of tensile residual stresses (Jedamski et al., 2020; Tönshoff et al.,1999). This allows for the non-destructive assessment of surface integrity, a critical requirement for fatigue-sensitive components.

2.2 Theoretical Background of Vibration Analysis

2.2.1 Context and Strategic Importance

To effectively harness vibration data, a strong theoretical foundation is essential. The translation of raw sensor signals—often complex and noisy—into actionable intelligence about the grinding process relies on established principles of signal processing and dynamic systems analysis. Understanding the fundamental concepts of time-domain, frequency-domain, and modal analysis is crucial for accurately identifying the sources of vibration, diagnosing process faults, and developing effective control strategies. This section establishes the theoretical framework that clarifies why specific vibrations occur and how they can be decoded, forming the basis upon which modern monitoring methodologies are built.

2.2.2 Principles of Vibration in Grinding

The vibrations encountered in grinding processes can be broadly categorized into two primary types, distinguished by their origin, dynamic characteristics, and industrial implications (Inasaki et al., 2001).

Forced Vibration: This type of vibration is caused by periodic external forces acting on the system. Common sources include eccentric force, unbalance force, and variations in the stiffness and damping of the grinding wheel spindle. As these vibrations are directly linked to machine components, their source can often be located by frequency measurement and subsequently suppressed through maintenance or component balancing (Inasaki et al., 2001).

Self-Excited Vibration (Chatter): This is a more complex and detrimental form of vibration that arises from an unstable, regenerative feedback loop within the cutting process. An initial vibration creates a wavy pattern on the grinding wheel surface. In subsequent rotations, this waviness modulates the cutting force, which in turn amplifies the vibration, reinforcing the pattern. This feedback loop can lead to a rapid escalation of vibration amplitude that will bring chatter marks to the workpiece. The frequency of chatter is typically close to a natural frequency of the mechanical system and should be avoided by setting appropriate grinding parameters (Inasaki et al., 2001).

Figure 2.2 demonstrates the vibrations in grinding processes.

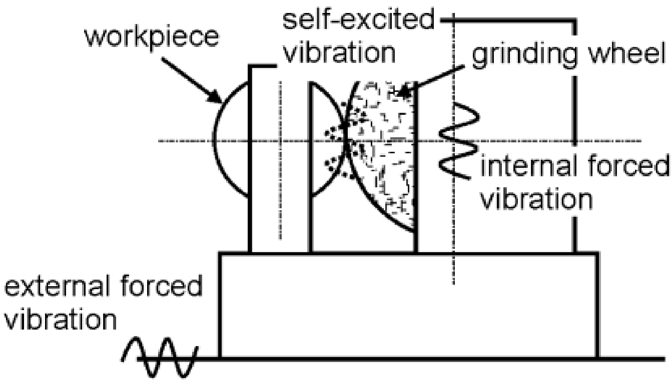

Figure 2.2: Chatter vibrations in grinding processes (Inasaki, 2001)

2.2.3 Core Analytical Concepts

2.2.3.1 Time-Domain Analysis

Time-domain analysis examines the kinematic behavior of system components by observing their amplitude and position over time. This approach is particularly useful for modeling the physical motion of individual elements within the grinding process. For instance, in studies of ultrasonic vibration-assisted grinding (UVAG), equations of motion are used to model the elliptical path of a single abrasive grain relative to the workpiece, providing insight into the mechanics of chip formation and material removal (Ahrens et al., 2014).

2.2.3.2 Frequency-Domain Analysis

Frequency-domain analysis deconstructs a complex time-series signal into its constituent frequencies, revealing dominant periodic patterns that are often hidden in the time-domain view. The Fast-Fourier-Transformation (FFT) is a cornerstone of this approach and is widely used to identify chatter. In an FFT spectrum of a chattering process, the vibration energy manifests at discrete peaks corresponding to the multiples of the wheel's rotation speed (Ahrens et al., 2014). Another powerful tool is the power spectral density function, which can be used to distinguish between different types of surface topography; surface waviness is typically represented by low-frequency components, while surface roughness is characterized by high-frequency components (Cui et al., 2025).

2.3. Applications of Vibration Signature Analysis in Grinding

2.3.1 Context and Strategic Importance

The practical application of vibration analysis has had a transformative impact on industrial grinding, providing solutions to long-standing challenges related to process stability, quality assurance, and optimization. By turning vibration data into actionable process improvements, these techniques demonstrate clear value, enabling higher productivity and more reliable manufacturing outcomes. This section reviews key case studies and applications from the literature that highlight the successful deployment of vibration signature analysis in real-world grinding scenarios.

2.3.2 Process Stability and Active Chatter Suppression

One of the most compelling applications of real-time vibration analysis is in the active suppression of chatter. Rather than simply avoiding chatter by using conservative parameters, active damping systems monitor the onset of instability and apply a counteracting force to stabilize the process. A notable case study by Ahrens et al. (2014) describes an active chatter damping system for plunge grinding. The system employs a "waviness observer," a real-time estimation algorithm that processes workpiece vibration data to model the developing waviness on the grinding wheel. This model is then used to predict the resulting regenerative process forces before they can destabilize the system, allowing a high-speed magnetic actuator to apply compensatory forces to the workpiece. This approach effectively cancels out the regenerative effect, preventing the growth of chatter and allowing the process to be run at higher material removal rates without sacrificing stability or surface quality.

2.3.3 Detection of Process Anomalies and Tool Wear

Vibration and related signatures serve as powerful tools for the real-time detection of process anomalies, including tool wear and thermal damage. This capability is fundamental to modern process monitoring and quality control.

Tool and Wheel Wear: Grinding force is a widely recognized indicator of the grinding wheel's condition. An increase in force signals can signify progressive abrasive wear or the adhesion of chips to the wheel surface, both of which degrade cutting performance and surface finish (Wu et al., 2023). Monitoring these force signatures allows for the timely intervention of dressing cycles, maintaining process consistency.

Thermal Damage (Grinding Burn): The non-destructive detection of grinding burn is a critical application, particularly for highly stressed components. Barkhausen noise analysis is effectively used for this purpose. An increase in the Barkhausen noise signal is correlated with a decrease in compressive residual stresses (or a shift toward tensile stresses) and a reduction in surface hardness—the classic microstructural signatures of thermal damage (Jedamski et al., 2020; Santa-aho et al., 2012). This allows for 100% in-process or near-process inspection, replacing destructive and environmentally hazardous methods like nital etching.

2.4. Research Gaps in Vibration Monitoring

2.4.1 Context and Strategic Importance

The successful implementation of vibration monitoring systems in an industrial grinding environment is often complicated by practical realities. The harsh conditions of the machining zone—characterized by high-pressure fluids, abrasive chips, and strong magnetic fields—present significant hurdles for data acquisition. Furthermore, the inherent complexity of the grinding process makes data interpretation a non-trivial task. A clear and realistic understanding of these challenges is crucial for developing robust, reliable, and industrially viable monitoring solutions that can transition from the laboratory to the factory floor.

2.4.2 Data Acquisition in Hostile Environments

The physical implementation of sensors in or near the grinding zone poses several primary challenges that can compromise signal quality and sensor longevity.

Sensor Protection: Sensors must be adequately shielded from the aggressive industrial environment. This includes protection from high-pressure metalworking fluids, abrasive chips, and strong magnetic interference from machine drives and actuators, which can corrupt sensitive electronic signals (Jedamski et al., 2020).

Sensor Wear: For techniques requiring direct or very close contact with the workpiece, such as certain Barkhausen noise probes, there is a significant risk of sensor wear, damage, or complete destruction due to the sliding contact with a rapidly rotating workpiece (Jedamski et al., 2020).

Signal Integrity: Acquiring clean, high-fidelity signals is often difficult due to the high levels of background process noise and the presence of stochastic, non-periodic defects. This noise can mask the underlying vibration signatures of interest, making it difficult to identify phenomena like the onset of chatter (Ahrens et al., 2014).

2.4.3 Complexity of Data Interpretation

Beyond the physical challenges of data acquisition, interpreting the collected data presents its own set of difficulties, rooted in the complexity of the process models and gaps in theoretical understanding.

For certain advanced measurement techniques, a complete theoretical framework linking the measured signal to the underlying physical properties is still being developed. It has been noted, for example, that for micromagnetic analysis, a "unified theory relating magnetic signals to basic magnetic parameters is lacking," which necessitates extensive, application-specific calibration procedures (Ducharne et al., 2023).

2.5. Recent Advancements and Future Trends

2.5.1 Context and Strategic Importance

The current landscape of innovation in grinding process monitoring is characterized by a distinct shift in focus. Driven by the principles of Industry 4.0, research and development efforts are moving away from a reliance on post-process inspection and toward the creation of intelligent, real-time, in-process control systems. The strategic importance of this evolution lies in its potential to embed sensing and analytics directly into the manufacturing process, enabling autonomous adaptation and optimization to ensure quality and efficiency without manual intervention.

2.5.2 Innovations in Real-Time Monitoring and Control

Recent literature highlights several cutting-edge systems that exemplify the trend toward real-time, closed-loop control. These innovations represent a significant step beyond simple process monitoring.

Active Damping Systems: As previously discussed, the development of active damping systems (Figure 2.3) represents a major innovation in real-time process control. By using a magnetic actuator to apply compensatory forces based on a real-time estimation of wheel waviness, these systems can actively suppress chatter as it begins to form, thereby stabilizing the process at much higher productivity levels than would otherwise be possible (Ahrens et al., 2014).

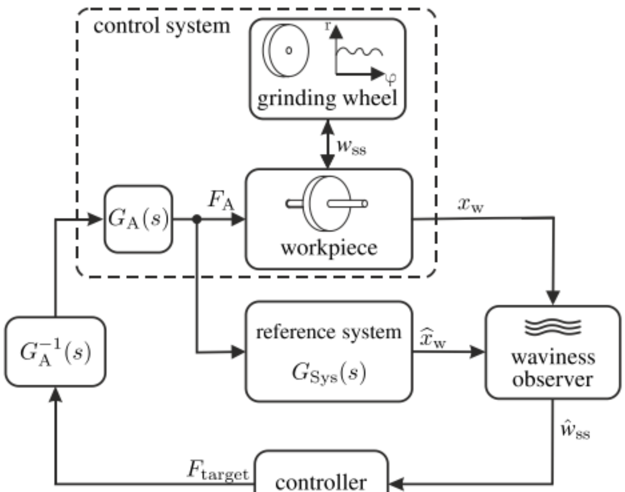

Figure 2.3: Active Damping System (Ahrens et al., 2014)

In-Process Surface Integrity Monitoring: The transition of Barkhausen noise analysis from a post-process laboratory technique to an in-process quality assurance tool marks a significant leap forward. The development of robust, protected sensor systems allows for real-time assessment of surface integrity during or immediately after the grinding cycle. This enables 100% inspection of critical surfaces for thermal damage like grinding burn, eliminating the delays and limitations of offline testing (Jedamski et al., 2020).

2.6 Conclusion

2.6.1 Synthesis of Key Findings

This literature review has affirmed the critical role of vibration monitoring in modern precision grinding, charting the field's evolution from problem identification to intelligent control. The fundamental industrial problem—unwanted vibrations degrading part quality and process efficiency—catalyzed the development of a robust theoretical understanding of vibration phenomena through time-domain, frequency-domain, and modal analysis. This theoretical framework enabled the creation of practical monitoring methodologies, which have progressed from direct measurement with simple sensors to sophisticated model-based estimation and indirect in-process systems. These methodologies have led to tangible industrial applications, most notably in active chatter suppression and the real-time detection of tool wear and thermal damage. Despite these successes, the field continues to grapple with persistent challenges, particularly the need for more durable sensors in hostile environments and the development of more generalizable data interpretation models, which in turn drive current and future research.

2.6.2 Implications for Future Research

The challenges and future trends identified in the literature present a clear roadmap for the research community. A primary focus should be the development of coupled, multi-physics models that integrate thermal, mechanical, and tribological factors for more holistic and accurate process simulation. Furthermore, a critical area of research will be the creation of computationally efficient yet accurate models that are suitable for deployment in real-time industrial control applications, bridging the gap between theoretical modeling and practical implementation.

2.6.3 Implications for Practical Application

For the manufacturing industry, the continued advancement and adoption of vibration signature analysis promises a fundamental transformation of the grinding process. The trajectory of innovation is moving grinding operations away from a reliance on operator experience and post-process quality checks and toward a highly automated, data-driven paradigm. The implementation of real-time, in-process monitoring and control systems will enable enhanced productivity through aggressive yet stable process parameters, coupled with guaranteed quality assurance. This evolution will ultimately lead to more efficient, reliable, and cost-effective manufacturing of high-precision components.

Chapter 3: Methodology

3.1 Introduction

This chapter discusses the experimental setup, equipment, stages, and methods employed to investigate the effect of magnetic field and ultrasonic frequency on the surface roughness of a cylindrical workpiece during grinding operation. The main objective of this chapter is to give a clear explanation of the research design so that the research findings can be independently validated. This chapter serves as the foundation of the research by explaining how and why of each methodological decision. The research follows a structured path where the results found from a number of experiments are used to draw a general conclusion regarding the effect of Magnetic Field Assisted grinding (MFAG) and Ultrasonic Vibration Assisted Grinding (UVAG) on surface roughness. The methodology is written in a way to be in consistent with the thesis's objectives: to measure any improvement by the application of these two unconventional grinding techniques (magnetic and ultrasonic) compared to the conventional one.

The whole research was conducted in 5 major steps. In the first step, cylindrical workpieces were selected for grinding, and conventional grinding was performed on one of them. The next step applied magnetic field by positioning a magnet at a fixed distance from workpiece and a constant depth of cut to compare the surface roughness with the conventional grinding and then magnet assisted grinding was performed at different magnet to workpiece distances and depth of cut to assess the effects of parameters on magnet assisted grinding. The third step used ultrasonic vibrations at different frequencies and constant depth of cut to compare surface roughness in ultrasonic assisted grinding with that in conventional grinding and then ultrasonic assisted grinding was performed further at different ultrasonic frequencies and depth of cut to experiment on the effects of parameters on ultrasonic assisted grinding. After each operation, surface roughness was measured. In the fourth step, ultrasonic assisted grinding was again performed at different ultrasonic frequencies, depth of cuts and workpiece RPM and the corresponding surface roughness values were collected. These parameters and surface roughness values were used to develop a quadratic mathematical model using Central Composite Design (CCD). The model was then validated by ANOVA. In the final step, desirability analysis was performed on the model to find the parameter values aimed at minimizing surface roughness. Figure 3.1 demonstrates the flowchart of the research.

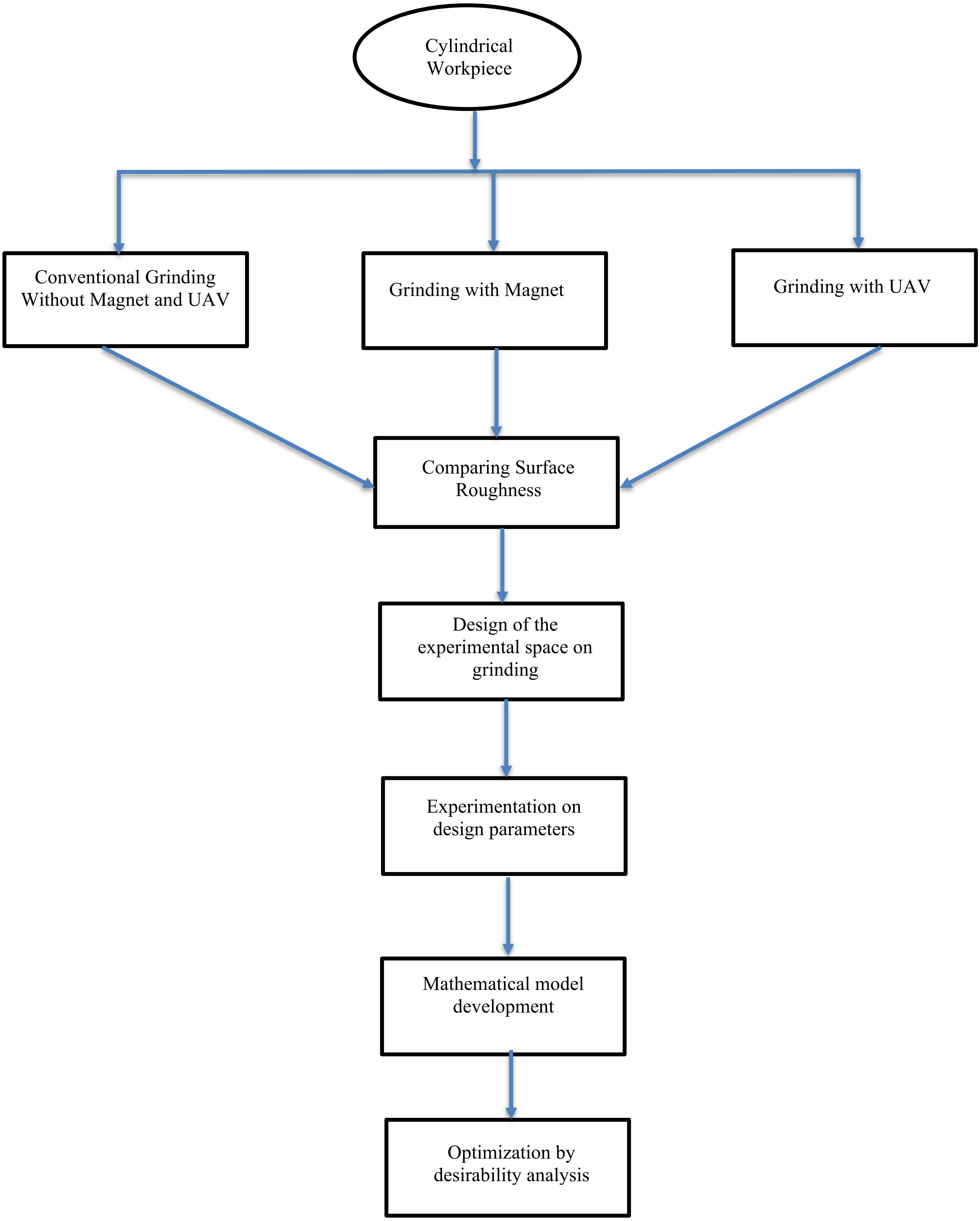

Figure 3.1: Flowchart of the research

3.2 Theoretical and Foundational Concepts

3.2.1 Conventional Cylindrical Grinding Principles

The experiment is based on the understanding of conventional cylindrical grinding. This process is characterized by four factors: rotation of the workpiece, rotation of the grinding wheel, radial feed of the wheel, and traversing of either the wheel or workpiece. Abrasive grains on the grinding wheel result in the removal of material from the workpiece.

3.2.2 Mechanism of Magnetic Field-Assisted Grinding (MFAG)

Applying a magnetic field in grinding results in significant differences from the conventional technique. The experimental setup used in this study is different from Magnetic Abrasive Finishing (MAF), where the finishing of the workpiece surface is done using a "magnetic brush" of abrasive particles (Zou & Shinmura, 2002). Static magnetic field is applied to the workpiece during the experiment.

The application of a magnetic field can affect grinding process in different ways. The ferromagnetic chips can be attracted by the magnetic field (Khan et al., 2013). This could result in the chips being attached to the workpiece and the grinding wheel, which in turn cause improper grinding operation and increased surface roughness (Khan et al., 2013).

Magnetic field can also cause mechanical strain in the workpiece by means of magnetostriction (ElBidweihy et al., 2013). If steels have positive magnetostrictive constant, magnetic amplitude is proportional to tensile stress and inversely proportional to compressive stress (Hristoforou et al., 2017; ElBidweihy et al., 2013). This affects chip formation and mechanical response to grinding force. Moreover, microstructure of steel is affected by high magnetic field, leading to improved grain of the material (Hurley et al., 2025).

The variance in the changing of magnet’s distance from the workpiece is for studying these factors. The study can investigate how these factors behave with the change of magnetic field strength as the strength of magnetic field will decrease with the increase of distance (Xu et al., 2024). Surface roughness is therefore the desired metric to assess the influences of these factors.

3.2.3 Mechanism of Ultrasonic Vibration-Assisted Grinding (UVAG)

In this method, high-frequency and low-amplitude vibrations are emitted on the workpiece. Due to this, the material removal method becomes a series of random small impacts between the workpiece and the abrasive grains, which is originally an uninterrupted and constant method of cutting operation (Jin et al., 2025). This greatly minimizes grinding force and the friction between the grinding wheel and the workpiece, leading to reduced heat in the grinding area (Jin et al., 2025). According to Li et al. (2024), this helps reduce damage by heat, residual stress, and microcracks on the surface of the workpiece. Though UVAG is used for hard and brittle materials, its application to ductile materials like mild steel is also useful. The vibrations in UAV help remove chips from the grinding area, which prevents the abrasive tool from becoming jammed and provides a stable and efficient process (Jin et al., 2025).

The research employs different levels of ultrasonic frequency. They will impact grinding force and will assist in determining an optimal frequency that demonstrates the least surface roughness. It will also give an insight of how ultrasonic vibration behaves on ductile materials like mild steel.

3.3 Materials and Experimental Equipment

3.3.1 Workpiece Material

For all the experiments, the workpiece material was made of mild steel. All the workpieces were 38 mm in diameter and 200 mm in length. The shape of the workpieces was cylindrical. Figure 3.2 shows the workpiece of the experiment.

Figure 3.2: Workpiece

3.3.2 Grinding Machine

All the operations were performed on Kondo Hi-Gloss-450 universal cylindrical grinding machine. The machine is shown in Figure 3.3.

Figure 3.3: Universal Cylindrical Grinding Machine

The specification of the grinding machine is shown in Table 3.1.

Table 3.1: Grinding Machine Specification

Component Name	Specification
Swing over table	250 mm
Length between center	450 mm
Max dia-ground with new wheel	150 mm
Max weight with new wheel	50 kg
Wheel width	16-75 mm
Wheel speed	1500 RPM
Grinding speed	2000 m/min
Wheel head- Traverse on screw	177 mm
Wheel head- Swivel	±30º
Wheel head- Fine feed	0.005
Table- Traverse	580 mm
Hydraulic traverse speed	10-2000 mm/min
Work head- Nose taper	MT-4

Work head- Spindle hole	26 mm
Work head- Spindle speeds	10-100, 50-500 RPM
Tailstock- Nose taper	MT-4
Tailstock- Spindle hole	20 mm
Tailstock- Travel	25 mm
Wheel head power	3.7 kW
Work head power	0.4 kW
Hydraulic pump power	0.75 kW
Lubrication pump power	0.1 kW
Coolant pump power	0.1 kW

3.3.3 Grinding Wheel

The grinding wheel was made of abrasive silicon and was a coarse type. The RPM of the grinding wheel had a constant value of 1500.

3.3.4 Magnet

A high-strength permanent magnet was used. The magnet was mounted on a holder, and this setup was positioned 2,3, and 4 mm from the workpiece for various operations. Figures 3.4 and 3.5 demonstrate the magnet with holder setup in front of the workpiece and the magnet, respectively.

Figure 3.5: Magnet

Figure 3.4: Magnet with holder setup

3.3.5 Ultrasonic Assisted Vibration (UAV)

The UAV had 2 sonotrodes for generating ultrasonic vibration. The sonotrodes were placed above the workpiece during the grinding operation. UAV and its setup with the grinding machine are shown in Figures 3.7 and 3.6.

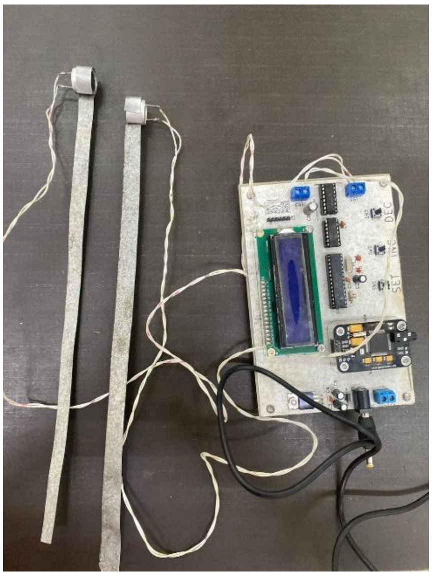

Figure 3.7: Ultrasonic Assisted Vibration

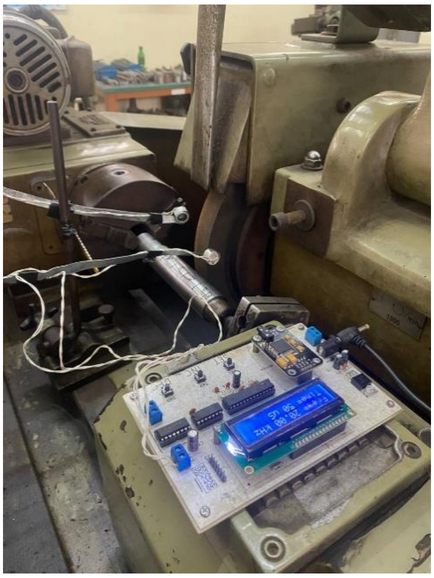

Figure 3.6: UAV setup on grinding machine

3.3.6 Surface Roughness Tester Machine

Surface roughness was measured using Mitutoyo Surftest SJ-210 surface roughness tester. The stylus of the machine was mounted in a stand and the workpiece was placed below the stylus to measure surface roughness. Figures 3.8 and 3.9 demonstrate the stand and surface roughness tester.

Figure 3.9: Surface Roughness Tester

Figure 3.8: Stand

The specification of the surface roughness tester machine is shown in Table 3.2.

Table 3.2: Surface Roughness Tester Machine Specification

Type of detector			Standard drive unit type		Retractable drive unit type	Transverse tracing drive unit type
Model No.			SJ-210 (0.75mN type)	SJ-210 (4mN type)	SJ-210 (4mN type)	SJ-210 (4mN type)
Order No.		inch/mm	178-561-01A	178-561-02A	178-563-02A	178-565-02A
Measuring range	X axis		.69" (17.5mm)			.22" (5.6mm)
	Z axis (Detector)	Range	14200 µin (-7900µin~+6300µin) / 360µm (-200µm ~ +160µm)			
		Range / Resolution	14170µin /.8µin (360µm / 0.02µm), 4000µin / .2µin (100µm / 0.006µm),1000µin /.08µin (25µm / 0.002µm)			
Measuring speed			Measuring: 0.01, 0.02, 0.03 in/s (0.25mm/s, 0.5mm/s, 0.75mm/s) Returning: 1mm/s			
Measuring force / Stylus tip			0.75mN type: 0.75mN / 2µmR 60°, 4mN type: 4mN / 5µmR 90°			
Skid force			Less than 400mN			
Applicable standards			JIS '82 / JIS '94 / JIS '01 / ISO '97 / ANSI / VDA			
Assessed profiles			Primary profile / Roughness profile / DF profile / Roughness profile-Motif			
Evaluation parameters			Ra, Rc, Ry, Rz, Rq, Rt, Rmax, Rp, Rv, R3z, Rsk, Rku, RPc, Rsm, Rmax, Rz1max, S, HSC, RzJIS, Rppi, RΔa, RΔq, Rlr, Rmr, Rmr(c), R δ c, Rk, Rpk, Rvk, Mr1, Mr2, A1, A2, Vo, Rpm, tp, Htp, R, Rx, AR, Possible Customize			
Analysis graphs			Bearing area curve / Amplitude distribution curve			
Filters			Gaussian, 2CR75, FC75			
Cut off length		λc	0.003, 0.01, 0.03, 0.1" (0.08 , 0.25 , 0.8 , 2.5mm)			
		λs	100, 300µin (2.5 , 8µm) or none			
Sampling length			0.003, 0.01, 0.03, .1 " (0.08 , 0.25 , 0.8 , 2.5mm)			
Number of Sampling lengths (xn)			x1,x2,x3,x4,x5,x6,x7,x8,x9,x10, Arbitrary 0.01~.63" (.0001" interval) [(0.3~16.0mm: 0.01mm interval)]			x1, x2, x3, x4, x5, x6, x7, x8, x9, x10, Arbitrary .0118 ~ .22" (.0001" Interval) [(0.3 ~ 5.6mm: 0.01mm Interval)]
LCD dimensions			1.45 x 1.93" (36.7×48.9 mm)			
Display languages			Japanese, English, German, French, Italian, Spanish, Portuguese, Korean, Traditional Chinese, Simplified Chinese, Czech, Polish, Hungarian, Turkish, Swedish, Dutch			
Calculation result display			Vertical display: 1 parameter / 3 parameter / trace to measurements Horizontal display: 1 parameter / 4 parameter / trace to measurements (Horizontal display is invertable)			
Printing function *1 (Dedicated printer is required separately.)			Measurement conditions / Calculation results / Calculation results for each sampling length / Assessed profile / Bearing area curve / Amplitude distribution curve / Environment setting information			
External I/O			USB I/F, Digimatic Output, Printer Output, RS-232C I/F, Foot SW I/F			
Functions	Customization		Desired parameters can be selected for calculation and display			
	GO / NG judgment *2		By max value / 16% / Standard deviation			
	Storage of measurement condition		Save the conditions at power OFF			
	Storage		Internal memory: Measurement condition (10sets), Measured profile (1set) Memory card (Option): 500 measurement conditions, 10000 measured profiles, 500 display images Text file (Measurement conditions / Measured profile / Assessed profile / Bearing area curve / Amplitude distribution curve)			
	Calibration		Saves last inputted nominal value of specimen / Average calibration with multiple measurement (Max.5 times) is available			
Power-saving function			Auto-sleep off function (10-600sec) *3			
Power supply			Two-way power supply: battery (rechargeable Ni-MH battery) and AC adapter *Charging time: about 4 hours (may vary due to ambient temperature) *Endurance: about 1000 measurements (differs slightly due to use conditions / environment)			
Size (WxDxH)		Display unit	2.05 x 2.6" x 6.3" (52.1×65.8×160mm)			
		Drive unit	4.5 x .9 x 1.02" (115×23×26mm)			
Mass			About 1.1lbs (500g) (Display unit + Drive unit + Standard detector)			
Standard accessories			**12BAA303** Connecting cable *4 **178-602** Roughness specimen (Ra 3.00µm) **12BAK699** Carrying case **12BAK700** Calibration stage **12BAK820** Protective sheets for display AC Adapter Operation manual Quick reference manual Warranty			**12BAA303** Connecting cable *4 **178-606** Roughness specimen (Ra 1.00µm) **12AAE643** Point-contact adapter **12AAE644** V-type adapter **12BAK699** Carrying case **12BAK700** Calibration stage **12BAK820** Protective sheets for display AC Adapter, Operation manual Quick reference manual, Warranty

*1: Order the SJ-210 printer (No.178-421A, optional accessory) separately.
See page 10 for details about the SJ-210 printer.
*2: Standard deviation only can be selected in ANSI. 16% rule cannot be selected in VDA.
*3: Auto-sleep function is invalid when AC adaptor is used.
*4: For connecting the calculation display unit and drive unit.

3.4 Process Parameters

The following tables summarize the key process parameters for all the experiments.

Table 3.3: Fixed Process Parameters

Workpiece material	Mild steel
Workpiece length	200 mm
Workpiece diameter	38 mm
Workpiece shape	Cylindrical
Grinding wheel material	Abrasive silicon
Grinding wheel type	Coarse
Grinding wheel RPM	1500
Fine feed	0

Table 3.4: Process Parameters for Initial Grinding Without Magnet, With Magnet, and With UAV

Workpiece RPM	120
Cross feed (DOC)	0.15
Magnet to workpiece distance	3 mm
UAV frequencies	20, 30, 40, 50 kHz

Table 3.5: Process Parameters for Magnet and Ultrasonic Assisted Grinding Under Varying Parameters

Magnet to workpiece distance	2, 3, 4 mm
UAV frequencies	20, 30, 40, 50, 60 kHz
Cross feed (DOC)	0.15, 0.2, 0.25
Workpiece RPM	120

Table 3.6: Process Parameters for Grinding with UAV for Mathematical Model Development

UAV frequencies	15, 20, 30, 50, 60 kHz
Cross feed (DOC)	0.05, 0.075, 0.1, 0.2, 0.25
Workpiece RPM	50, 60, 120, 250, 360

3.4 Experimental Sequence

Conventional Grinding: The first experiment was a conventional experiment without the presence of magnet and UAV. This experiment was done to use the resulting surface roughness of this operation as a baseline for comparison.

Magnet Assisted Grinding: After the completion of conventional grinding, grinding operations were performed with magnet. The magnet was placed 3 mm from the workpiece. All the other process parameters were the same as those in conventional grinding. After this operation, several grinding operations were done again with magnet under various levels of magnet-to-workpiece distance and depth of cut. These grinding operations were done to assess how grinding in the presence of magnetic field affects surface roughness of the workpiece and how several process parameters along with magnet causes variations in surface roughness.

Ultrasonic Assisted Grinding: Following grinding with magnet, grinding operations were done with the presence of ultrasonic frequency in two steps. In the first step, ultrasonic frequencies of 20,30,40,50 kHz were used and other process parameters remained same as conventional grinding. The aim was to observe how much ultrasonic frequency improves grinding. The second step employed varied levels of depth of cut along with ultrasonic frequency. These operations were done to measure the effects of different process parameters on surface roughness.

Final Stage of Ultrasonic Assisted Grinding: Finally, a series of grinding operations was done with UAV under different magnitudes of ultrasonic frequency, depth of cut, and workpiece RPM. These operations were performed to build a mathematical model using Central Composite Design (CCD).

Mathematical Model Development: A quadratic mathematical model was established from the CCD. The model was validated using ANOVA. Predicted vs Actual plot was constructed based on the mathematical model to visualize the model's accuracy, and 3D response surface plots were constructed to visualize multiple factors' effect on surface roughness together.

Optimization with Desirability Analysis: Based on the quadratic model, desirability function analysis was performed with the aim of optimizing the grinding process. The objective of this was to minimize the surface roughness by determining the corresponding parameters' values.

3.5 Data Collection

Data was collected by the surface roughness tester machine after each operation. For each workpiece, surface roughness was measured three times, and their average was calculated for the final value of surface roughness. This was done to avoid any large variation in the measurement. The surface roughness parameter was the arithmetic average roughness (R_a).

Figure 3.10: Measuring surface roughness

3.7 Limitations and Mitigations

Every study and research has its limitations, and this research is also not exceptional. MFAG has the possibility of residual magnetism in the workpiece and the grinding wheel (Khan et al., 2013). Chip will remain on the workpiece due to this residual magnetism, which can affect the measurement (Khan et al., 2013). The residual magnetism effect could not be totally reduced despite changing of workpieces in each operation.

Another limitation is tool wear. Grinding process causes wear of abrasive grain on grinding wheel, which affects surface roughness.

Finally, grinding generates heat on the contact surface during the operation. Because of this, the workpiece experiences residual stresses and microstructural changes (Hristoforou et al., 2017; ElBidweihy et al., 2013).

3.8 Summary

This chapter provided the methodology for experimenting with the effect of magnetic field and ultrasonic frequency in cylindrical grinding. The selected workpieces were all made of mild steel and 200 mm in length and 38 mm in diameter. The experiments were conducted on a cylindrical grinding machine under constant grinding wheel RPM of 1500 and fine feed of 0. Magnet and ultrasonic assisted grinding were performed in several stages to first compare them with conventional grinding and then to examine the effects of the parameters on grinding. The final step was to build a mathematical model using Central Composite Design to understand how several parameters affect surface roughness and to optimize grinding process using desirability analysis.

Chapter 4: Results and Discussions

4.1 Introduction

This chapter demonstrates and discusses the results and mathematical model established from the experiments. The results from the experiments were analyzed to understand the effects of process parameters on surface roughness. These results were used to develop a quadratic equation model using Central Composite Design (CCD) and validating it by Analysis of Variance (ANOVA). Desirability function analysis was employed for process optimization and finding the best combinations of process parameters to obtain the minimum surface roughness possible.

4.2 Conventional Grinding

Table 4.1 summarizes the resulting surface roughness in the grinding operation without magnet and ultrasonic frequency. Workpiece RPM was 120 and depth of cut was 0.15 during the experiment.

Table 4.1: Surface Roughness in Conventional Grinding

Surface Roughness (R_a) Before Grinding (µm)	Surface Roughness (R_a) After Grinding (µm)	% of Surface Roughness Reduction
3.807	2.548	33.7

This confirmed that grinding process improves the surface quality of materials. This operation was set baseline to compare it with grinding in the presence of magnet and ultrasonic frequency. Figures 4.1 and 4.2 demonstrate the surfaces before and after grinding, respectively.

Figure 4.1: Workpiece surface before grinding

Figure 4.2: Workpiece surface after grinding

4.3 Magnetic Field Assisted Grinding

The first step of grinding under magnet employed workpiece RPM of 120 and 0.15 depth of cut. Magnet to workpiece distance was 3 mm. Table 4.2 summarizes the results.

Table 4.2: Surface Roughness in MFAG at Constant Magnet to Workpiece Distances and DOC

Surface Roughness (R_a) Before Grinding (µm)	Surface Roughness (R_a) After Grinding with Magnet (µm)	% of Surface Roughness Reduction
3.807	2.46	35.38

From the results, grinding in the presence of magnet caused greater R_a reduction (35.38%) than in conventional grinding (33.7%). This can be interpreted that magnetic field in grinding improves surface roughness.

Figure 4.3 shows the workpiece surface after grinding with magnet.

Figure 4.3: Workpiece surface after grinding with magnet

The next step of grinding under magnet employed different levels of magnet to workpiece distances and depth of cuts and a constant workpiece RPM 120. Table 4.3 summarizes the results:

Table 4.3: Surface Roughness in MFAG at Different Magnet Distances and DOC

Magnet to Workpiece Distance (mm)	**Surface Roughness (µm) (0.15 DOC)**	**Surface Roughness (µm) (0.2 DOC)**	**Surface Roughness (µm) (0.25 DOC)**
2	2.727	3.757	4.82
3	3.604	4.413	5.089
4	4.158	3.232	4.858

The obtained data showed complex relationships between the magnet to workpiece distance, depth of cut, and surface roughness. There is a clear pattern that, under constant magnet to workpiece distance, surface roughness increases with the increase in depth of cut (DOC). For example, at a 2 mm distance, surface roughness is 2.727 µm at 0.15 DOC and 4.82 µm at 0.25 DOC, resulting in almost 77% deterioration in surface roughness. This is supported by grinding theory, as higher DOC causes higher grinding force and higher material removal rate and creates deeper grooves on the workpiece surface (Malkin & Guo, 2008).

Magnet distance exhibited a more complex pattern. The best surface roughness of them was 2.727 µm at 2 mm magnet distance and 0.15 DOC, but at higher DOC, such as 0.2, 4 mm magnet distance exhibited better surface roughness compared to 2 mm and 3 mm distances on the same DOC. This can be interpreted as other cutting parameters impacting the magnetic field for surface finish. Applying magnetic field to a ferromagnetic material like mild steel can have two opposing consequences: the ferromagnetic chip will be attracted by the workpiece, which worsens surface finish (Khan et al., 2013), and the possibility of a positive magnetoelastic effect on the microstructure of the workpiece (Hristoforou et al., 2017; ElBidweihy et al., 2013). The results suggest that the advantages of magnetic assisted grinding exceed the disadvantages of it at a specific magnet to workpiece distance and depth of cut. The change in surface roughness at different magnet to workpiece distances and depth of cuts is visualized in Figure 4.4.

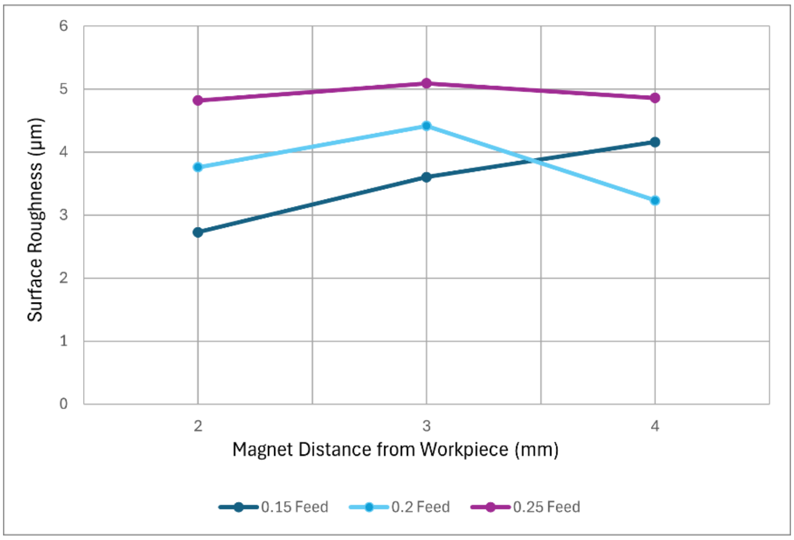

Figure 4.4: Variation of surface roughness at different magnet distances and depth of cut

Table 4.4 demonstrates the images of surfaces for the operations in Table 9.

Table 4.4: Workpiece Surface Images in MFAG at Different Magnet Distances and DOC

Magnet to Workpiece Distance (mm)	0.15 DOC	0.2 DOC	0.25 DOC
2			
3			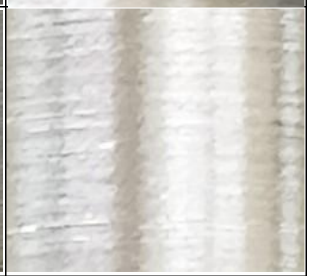
4			

4.4 Ultrasonic Vibration Assisted Grinding

The first step of ultrasonic assisted grinding employed grinding at different ultrasonic frequencies under a constant workpiece RPM of 120 and 0.15 depth of cut. Table 4.5 summarizes the results:

Table 4.5: Surface Roughness in UVAG at Constant Feed

Ultrasonic Frequency (kHz)	Surface Roughness (R_a) µm	% Roughness Decrease
0 (Initial)	4.667	0
20	3.179	31.88
30	3.568	23.54
40	3.0083	35.54
50	3.204	31.35

From the above results, all the ultrasonic frequencies except 40 kHz showed a lower surface roughness reduction rate (31.88% for 20 kHz, 23.54% for 30 kHz, and 31.35%) than in conventional grinding (33.7%). Only 40 kHz exhibited a higher reduction rate (35.54%) than conventional grinding. This can be explained that higher grinding performance in the presence of ultrasonic vibration is frequency specific. This important finding led to a deeper study of ultrasonic assisted grinding and, as a result, more testing phases. Figure 4.5 illustrates how surface roughness changes with the increase of ultrasonic frequency.

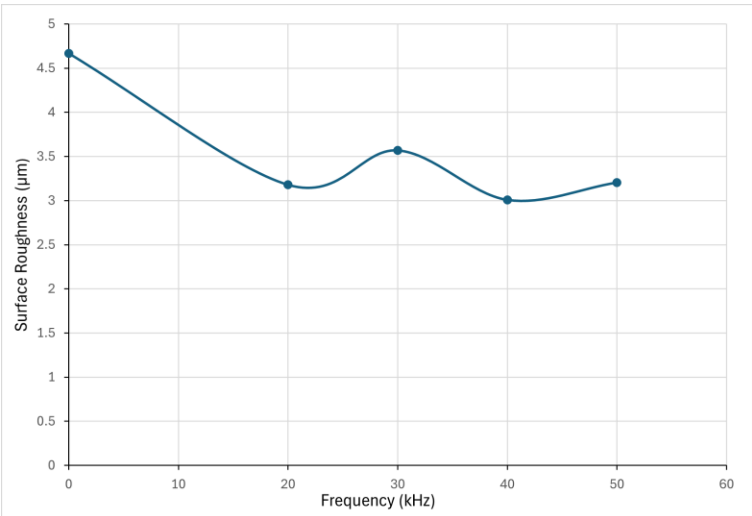

Figure 4.5: Variations of surface roughness at different ultrasonic frequencies

Figure 4.6 demonstrates the workpiece surfaces after performing grinding operation.

(a) 20 kHz **(b)** 30 kHz **(c)** 40 kHz **(d)** 50 kHz

Figure 4.6: Workpiece surfaces of grinding at different frequencies

The second step of ultrasonic vibration assisted grinding involved grinding at varying levels of ultrasonic frequencies and depth of cuts and constant workpiece RPM of 120. The following Table 4.6 summarizes the results:

Table 4.6 Surface Roughness in UVAG at different frequencies and DOC

UAV Frequency (kHz)	Surface Roughness (µm) (0.15 DOC)	Surface Roughness (µm) (0.2 DOC)	Surface Roughness (µm) (0.25 DOC)
20	3.179	3.165	3.462
30	3.568	3.28	4.118
40	3.0083	3.288	2.904
50	3.204	4.642	3.864
60	3.176	4.374	3.83

There is a common pattern in the change of surface roughness with respect to ultrasonic frequency and depth of cut. At every constant feed value, surface roughness rapidly increased while increasing ultrasonic frequency from 20 kHz to 30 kHz, then surface roughness sharply decreased and reached its lowest at 40 kHz frequency, and then again suddenly increased, as shown in Figure 4.7.

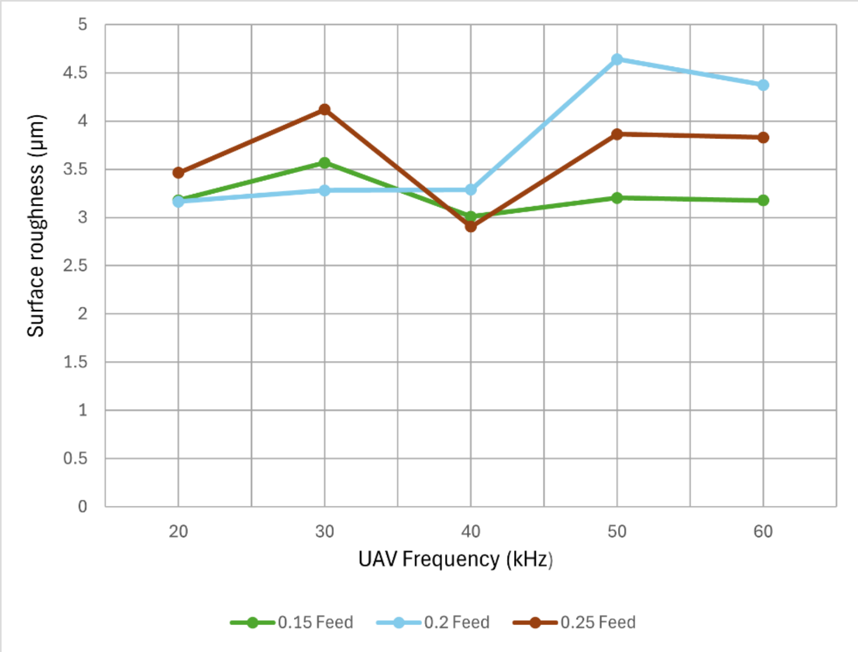

Figure 4.7: Variation of surface roughness at different ultrasonic frequencies and depth of cuts

The lowest value of surface roughness obtained was 2.904 µm at 40 kHz and 0.25 DOC. In every feed, 40 kHz frequency providing the best surface finish may indicate a potential resonance effect at this frequency, where the grinding dynamics and vibration frequency interact with each other to form chip effectively and reduce grinding forces (Brehl & Dow, 2008). Table 4.7 shows the resulting workpiece surface images in the second step ultrasonic assisted grinding.

Table 4.7: Workpiece Surface Images in UVAG at different frequencies and DOC

UAV Frequency (kHz)	Surface Roughness (µm) (0.15 DOC)	Surface Roughness (µm) (0.2 DOC)	Surface Roughness (µm) (0.25 DOC)
20			
30			
40			
50			
60	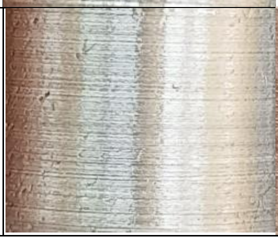		

4.5 Mathematical Model Development Using Central Composite Design

To build a predictive mathematical model, Central Composite Design (CCD) method was utilized by using three factors: UAV frequency (A), depth of cut/feed (B), and workpiece RPM (C). CCD in Response Surface Methodology (RSM), used for fitting second-order polynomial models, enables the estimation of curvature effects with fewer runs than a full factorial design. Randomization and blocking were used in CCD to increase the validity and precision of the model (Montgomery, 2017). The response variable used was the natural logarithm of surface roughness, Ln(R_a), to make the variance stable and improve model fit (Box et al., 2005). The experiment used total 15 experimental runs, and among them 5 repeated runs for the center points.

The experimental runs were executed in random order, as shown by the "Random Runs" column in the design matrix (Table 4.9). This is required to ensure that the observed effects are caused by the manipulated parameters and to prevent time-related trends (such as machine warm-up, tool wear, and environmental changes) from being confused with the variables' primary impacts (Box et al., 2005).

The experiment was divided into two blocks. Block 1 was formed with factorial and center points and and Block 2 was formed with axial points. This blocking is a common technique in CCD to prevent the modification of the estimation of pure error and quadratic terms from variability that might arise between different time periods (Myers, Montgomery, & Anderson-Cook, 2016).

The three input factors and their coded levels are shown in Table 4.8.

Table 4.8: Coded Values for UAV, DOC and RPM

	Coding				
Parameters	-1.414	-1	0	1	1.414
UAV	15	20	30	50	60
DOC	0.05	0.075	0.1	0.2	0.25
RPM	50	60	120	250	360

Table 4.9 demonstrates the combinations of input parameters in each experimental run and the resulting output response (surface roughness).

Table 4.9: Central Composite Design Matrix

Standard Runs	Random Runs	Blocks	UAV	Feed	RPM	R_a (µm)
1	2	Block 1	1	1	-1	4.942
2	6	Block 1	1	-1	1	3.117
3	1	Block 1	-1	1	1	4.117
4	5	Block 1	-1	-1	-1	4.972
5	3	Block 1	0	0	0	3.477
6	9	Block 1	0	0	0	3.552
7	7	Block 1	0	0	0	3.526
8	8	Block 1	0	0	0	3.441
9	4	Block 1	0	0	0	3.492
10	13	Block 2	-1.414	0	0	3.875
11	14	Block 2	1.414	0	0	4.595
12	10	Block 2	0	-1.414	0	4.46
13	15	Block 2	0	1.414	0	4.564
14	11	Block 2	0	0	-1.414	4.074
15	12	Block 2	0	0	1.414	2.909

4.5.1 Model Selection

A sequential model sum of squares analysis was performed to determine the most significant and appropriate model. In this analysis, linear, two-factor interaction (2FI), quadratic, and cubic models were tested for their significance. Table 4.10 summarizes the results:

Table 4.10: Sequential Model Sum of Squares

Source	Sum of Squares	DF	Mean Square	F Value	Prob > F	
Mean	26.13	1	26.13	–	–	
Block	1.393E-003	1	1.393E-003	–	–	
Linear	0.17	3	0.057	2.54	0.1222	
2FI	0.045	3	0.015	0.58	0.6477	
Quadratic	0.15	3	0.052	132.84	0.0011	Suggested
Cubic	6.392E-004	1	6.392E-004	2.43	0.2592	Aliased
Residual	5.254E-004	2	2.627E-004	–	–	
Total	26.51	14	1.89	–	–	

The linear, 2FI, and cubic models are not significant due to their p values > 0.05. The cubic model is aliased which means that the experimental design does not have enough unique runs to independently estimate all the cubic terms. On the other hand, the quadratic model is significant ($p < 0.05$) and a high F value of 132.84 suggests a better fit for the data. Therefore, the quadratic model is selected due to its ability to fit data and capture the complex patterns of response surface.

4.5.2 Analysis of Variance (ANOVA) of the Quadratic Model

ANOVA was done on the quadratic model to assess the significance of the terms in the model and also the model itself. The ANOVA table is shown in Table 4.11.

Table 4.11: Analysis of Variance Table (Partial Sum of Squares)

Source	Sum of Squares	DF	Mean Square	F Value	Prob > F	
Block	1.393E-003	1	1.393E-003	–	–	
Model	0.37	9	0.041	105.99	0.0014	Significant
A	0.015	1	0.015	37.41	0.0088	
B	2.657E-004	1	2.657E-004	0.68	0.4688	
C	0.057	1	0.057	146.11	0.0012	
A^2	0.055	1	0.055	141.89	0.0013	
B^2	0.11	1	0.11	271.21	0.0005	
C^2	1.472E-003	1	1.472E-003	3.79	0.1466	
AB	3.735E-003	1	3.735E-003	9.62	0.0532	
AC	7.152E-003	1	7.152E-003	18.42	0.0233	
BC	0.035	1	0.035	89.99	0.0025	
Residual	1.165E-003	3	3.882E-004	–	–	
Lack of Fit	6.392E-004	1	6.392E-004	2.43	0.2592	Not significant
Pure Error	5.254E-004	2	2.627E-004	–	–	
Cor Total	0.37	13	–	–	–	

The high F value (105.99) and low p value (0.0014) indicate that the quadratic model is very significant and can explain variations in data. There is only a 0.14% chance that such an F-value could occur due to noise. Low sum of squares values of block (1.393E-003) indicates the block effect is insignificant and there is negligible variation between the two experimental blocks.

The ANOVA table reveals that workpiece RPM (C) is the most significant factor as having the lowest p value (0.0012) among the three factors, where a high p value (0.4688) of factor B (DOC) shows that it is the least significant factor in determining the output response (surface roughness). The high p value of quadratic terms A^2 and B^2 confirms a strong nonlinear relationship between the variables. The effects of interaction terms ultrasonic frequency and workpiece RPM (AC), and DOC and workpiece RPM (BC) are also significant (p=0.0233 and p=0.0025, respectively), which points out that the effect of one parameter depends on the level of the other (Myers, Montgomery, & Anderson-Cook, 2016).

The non-significance of "Lack of fit" (p=0.2592) is expected because it confirms that the model is enough to explain the variation in data, and a more complex model than this is not required (Montgomery, 2017).

From the above analysis, the quadratic model of predicting surface roughness in terms of coded factors is,

$$Ln(R_a) = +1.25 + 0.060 * A + 8.150E\text{-}003 * B - 0.12 * C + 0.087 * A^2 + 0.12 * B^2 - 0.014 * C^2 + 0.043 * A * B - 0.060 * A * C + 0.13 * B * C$$

The negative coefficient of the factor C (workpiece RPM) emphasizes its crucial role on surface finish (Marinescu et al., 2016). The positive coefficients for the quadratic terms A^2 and B^2 indicate a nonlinear, U-shaped relationship.

4.5.3 Model Diagnostics and Response Surface Analysis

4.5.3.1 Predicted vs Actual and Perturbation Plot

Figure 4.8 illustrates the predicted vs actual surface roughness plot based on the experimental values and the predictive model. The diagonal straight line is the line obtained from the quadratic equation, and the individual data points are the experimental surface roughness values. The plot shows little variation between the theoretical and experimental values. The clustering of experimental data points around the ideal straight line indicates the model is highly accurate throughout the design space.

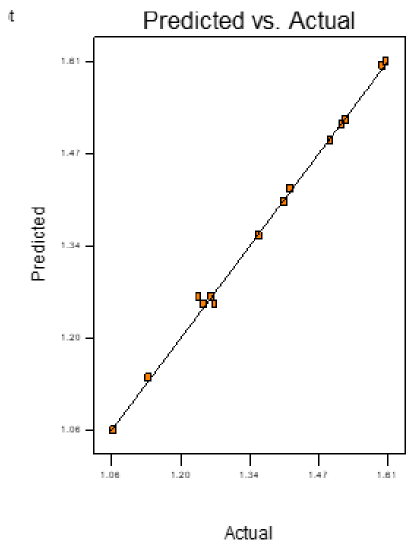

Figure 4.8: Predicted vs Actual surface roughness plot

The perturbation analysis plot in Figure 4.9 explains how each factor (Ultrasonic frequency, depth of cut, and workpiece RPM) has individual effects on the output response (surface roughness). Among the three factors, C (workpiece RPM) has the steepest negative slope, which again proves its dominance on the surface roughness values. The C curve indicates that surface roughness decreases with the decrease in workpiece RPM. Unlike workpiece RPM, factors A (Ultrasonic frequency) and B (DOC) exhibited more nonlinear relationships with surface roughness, and they show the best result at specific optimal ranges. Surface roughness slowly decreases with the decrease of ultrasonic frequency and then suddenly increases with the increase of frequency. Curve B (DOC) is almost U-shaped, and similar to ultrasonic frequency, initially increasing it decreases surface roughness and reaches a minimum, and then again surface roughness increases, but curve B has a less steep positive slope compared to curve A.

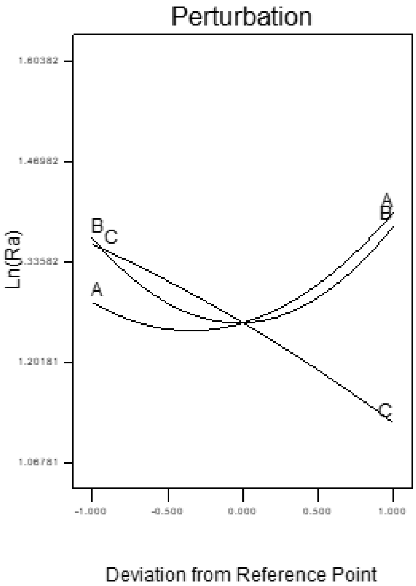

Figure 4.9: Perturbation analysis plot

4.5.3.2 3D Response Surface Plots

The 3D response surface plot describes how multiple factors together affects an output response. Figure 4.10 illustrates the combined effects of ultrasonic frequency and DOC on surface roughness. This shows almost a bowl-shaped surface. Surface roughness exhibits the highest value (4.83 µm) at the highest value of ultrasonic frequency (50 kHz) and DOC (0.25). The optimum (lowest) surface roughness is found at around 30 kHz frequency and 0.1 DOC.

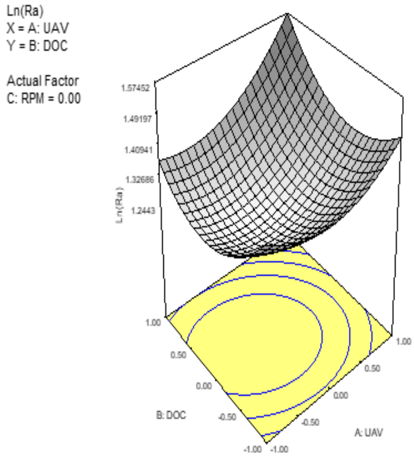

Figure 4.10: 3D Response surface plots of Ln(Ra) vs DOC vs UAV

The combined effects of ultrasonic frequency and workpiece RPM are shown in the 3D response surface in Figure 4.11. The response surface here is like a curved flat surface. In this response surface, the highest surface roughness (4.79 µm) is obtained at 60 kHz ultrasonic frequency, 60 RPM, and at 20 kHz frequency, 60 RPM. The optimum (lowest) value of surface roughness is at around 250 RPM and 30 kHz frequency.

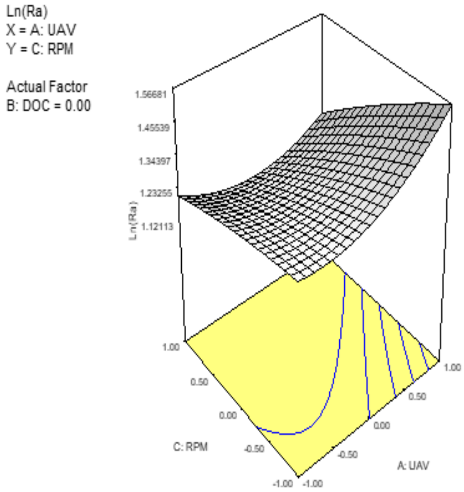

Figure 4.11: 3D response surface plot of Ln(Ra) vs RPM vs UAV

4.6 Optimization by Desirability Analysis

Desirability function analysis was utilized to determine the optimized grinding parameters and minimize surface roughness (Derringer & Suich, 1980). In this process, the output response variable, here Ln(Ra) is converted to a desirability value ranging from 0 (undesirable) to 1 (fully desirable). This optimization algorithm aims to maximize the overall desirability D and find the best factor setting (frequency, depth of cut, workpiece RPM) so that the main goal of minimizing the output response (surface roughness) can be satisfied (Myers et al., 2016).

Table 4.12 summarizes the results obtained by desirability function analysis.

Table 4.12: Desirability Function Analysis

Name	Goal	Lower Limit	Upper Limit	Lower Weight	Upper Weight	Importance
UAV	is in range	-1.414	1.414	1	1	3
DOC	is in range	-1.414	1.414	1	1	3
RPM	is in range	-1.414	1.414	1	1	3
Ln(R_a)	minimize	1.06781	1.60382	1	1	4

Solutions Number	UAV	DOC	RPM	Ln(R_a)	Desirability	
1	0.18	-0.15	1.26	1.059	1.00	Selected
2	0.47	-0.53	1.11	1.064	1.00	

From Table 4.12, the optimal solutions to get the lowest surface roughness are the coded values of ultrasonic frequency, depth of cut, and workpiece RPM of 0.18, -0.15, 1.26, respectively. Converting their values, they are 31.8 kHz, 0.092, and 336 RPM, respectively.
Together, they result in the lowest Ln(Ra) value of 1.059, which converted to R_a is 2.88 µm.

Figure 4.12 illustrates the desirability optimization plots.

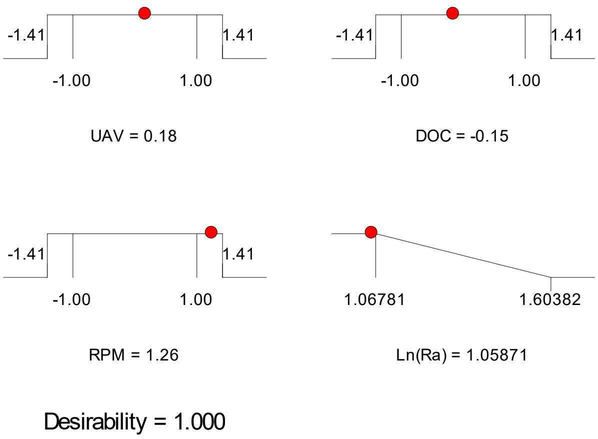

Figure 4.12: Desirability optimization plots

4.7 Summary

This chapter provided a detailed and comprehensive analysis and investigation of the magnetic and ultrasonic assisted grinding's advantages over conventional grinding and a quadratic mathematical model to predict surface roughness in ultrasonic assisted grinding.

The study started with conventional grinding in order to establish a baseline for comparison. The conventional grinding showed 33.7% surface roughness reduction. Magnet assisted grinding in the first step at constant magnet to workpiece distance and DOC showed 35.38% surface roughness reduction, confirming its efficiency over conventional grinding. The second stage of magnet assisted grinding at varying magnet to workpiece distances and DOC resulted the lowest surface roughness of 2.727 µm at 2 mm magnet to workpiece distance and 0.15 DOC, which were the lowest distance and DOC values, but at some higher DOC, maintaining a higher magnet distance worked well on surface finish than at a lower magnet distance in that same DOC.

Ultrasonic assisted grinding in the first stage at constant DOC showed the highest 35.54% surface roughness reduction at 40 kHz. Further experiments in the second stage at varying DOC also suggested the lowest surface roughness (2.904 µm) at 40 kHz. This can be interpreted as applying ultrasonic vibrations improves surface roughness at a specific ultrasonic frequency range.

The final task was to build a mathematical model by employing the Central Composite Design (CCD) method with 15 total experimental runs, including 5 repeated runs for repeatability analysis. A quadratic model was suggested by the CCD analysis, which was further validated by ANOVA. The ANOVA also emphasized workpiece RPM as the most significant factor in predicting surface roughness. The Actual vs Predicted plot further confirmed the model's validity and accuracy, and the Perturbation plot visualized each individual factor's effect on surface roughness, where surface roughness decreases with the decrease of workpiece RPM and surface roughness is minimum at a specific range of ultrasonic frequency and depth of cut. These relationships were further illustrated by 3D response surface plots.

Finally, desirability function analysis was done to optimize the grinding parameters and to achieve the lowest surface roughness value possible. The analysis converged to an overall desirability of 1 for the setting of ultrasonic frequency: 31.8 kHz, DOC: 0.092 mm, and workpiece RPM: 336. In this setting, 2.88 μm surface roughness is predicted by the model.

Chapter 5: Conclusions and Future Recommendations

5.1 Introduction

This final chapter serves to synthesize the entirety of the research presented in this thesis. It begins by re-establishing the core research problem and objectives that motivated this investigation, thereby grounding the conclusions in the study's original purpose. Following this recapitulation, the chapter distills the principal findings derived from the experimental investigations into conventional, Magnetic Field-Assisted Grinding (MFAG), and Ultrasonic Vibration-Assisted Grinding (UVAG) processes. This structured summary provides a comprehensive overview of the research outcomes before their broader implications are explored.

5.1.1 Recapitulation of Research Problem and Aim

The central challenge addressed by this research originates from a critical industrial need to control process anomalies in precision grinding, a finishing operation paramount to modern manufacturing. Phenomena such as self-excited vibrations (chatter) and thermal damage are significant limiting factors that can compromise component quality, reduce productivity, and cause damage to manufacturing equipment. While the necessity for process monitoring is well-established, a significant research gap exists in the form of a need for a robust, non-invasive, and real-time monitoring technique capable of simultaneously diagnosing multiple process anomalies from a unified signal source. Existing methods are often specialized, failing to provide the holistic view required for comprehensive process control.

The premise of this research was that process vibration, as a direct physical manifestation of the underlying machining mechanics, contains the rich, high-frequency information necessary to fill this gap. The primary aim of this research was to identify and analyze characteristic vibration signatures in the grinding process to serve as a diagnostic tool for real-time condition monitoring.

To achieve this aim, the following specific objectives were established:

1. To investigate how magnetic field and ultrasonic frequency affect the grinding process by measuring surface roughness.
2. To build a mathematical model on how different process parameters affect surface roughness in ultrasonic vibration assisted grinding.

3. To propose a new method of grinding using magnet and ultrasonic vibration.

5.1.2 Synthesis of Key Experimental Findings

The experimental investigations detailed in Chapter 5 yielded several critical findings that directly address the research objectives. These principal outcomes are summarized below:

- **Baseline Performance:** Conventional cylindrical grinding established the performance benchmark for this study. The process achieved a 33.7% reduction in the initial surface roughness (Ra) of the mild steel workpiece, providing a quantitative baseline against which advanced techniques were compared.
- **Magnetic Field-Assisted Grinding (MFAG) Analysis:** The application of a static magnetic field demonstrated the potential to improve surface finish beyond conventional methods. Under specific conditions (3 mm magnet-to-workpiece distance), MFAG achieved a superior surface roughness reduction of 35.38%. However, the investigation revealed a complex relationship between process parameters. Surface roughness consistently increased with a higher depth of cut (DOC), while the effect of magnet distance was non-linear. This suggests a trade-off between the beneficial magnetoelastic effects on the workpiece microstructure and the detrimental effects of ferromagnetic chip adhesion to the workpiece and wheel, which can degrade surface quality.
- **Ultrasonic Vibration Assisted Grinding (UVAG) Analysis:** The study revealed that the effectiveness of UVAG is highly frequency-specific. While several frequencies were tested, a frequency of 40 kHz yielded the best performance, achieving a surface roughness reduction of 35.54%, which surpassed both conventional grinding and the initial MFAG test. This finding indicates a resonance effect, where the applied ultrasonic frequency interacts constructively with the system's natural dynamics to optimize chip formation and reduce grinding forces, as suggested by Brehl and Dow (2008).

Predictive Model Development and Optimization: A key outcome of this research was the successful development of a predictive quadratic model for the UVAG process using Central Composite Design (CCD). Analysis of Variance (ANOVA) confirmed the model's

- statistical significance ($p < 0.05$) and identified workpiece RPM as the most influential factor impacting surface roughness. Subsequent optimization using desirability function analysis determined the optimal parameters for minimizing surface roughness to be a 31.8 kHz frequency, 0.092 DOC, and 336 RPM. Under these conditions, the model predicted a minimum achievable surface roughness (Ra) of 2.88 μm.

These findings provide a clear, evidence-based understanding of how advanced assistance techniques can modify grinding dynamics, leading directly to a discussion of their broader implications for the field.

5.2 Implications of the Study

Moving beyond a summary of the experimental results, this section evaluates the theoretical contributions and practical applications of the research. By contextualizing the findings within both academic discourse and industrial practice, it establishes the overall value and significance of the study.

5.2.1 Theoretical Implications

This research contributes to the academic understanding of advanced grinding processes by providing empirical evidence for complex physical phenomena. The frequency-specific success of UVAG, with optimal performance observed at 40 kHz, lends strong empirical support to the concept of process resonance. While the concept of resonance is established, this study provides a specific, empirically validated frequency (40 kHz) for this material-tool system, transitioning the concept from a theoretical possibility to an actionable process parameter (Brehl & Dow, 2008).

Furthermore, the complex and non-linear results observed in the MFAG experiments challenge simplistic models of the process and underscore the necessity of multi-physics models that can account for competing effects. The data provide a quantitative basis for modeling the trade-off between beneficial magnetoelasticity and detrimental chip adhesion dynamics, moving beyond a qualitative acknowledgment of a "delicate balance" (Khan et al., 2013). This empirical validation of competing phenomena enriches the theoretical models used to describe magnetically assisted machining.

5.2.2 Practical and Industrial Implications

The practical implications of this study are demonstrated by the development of the predictive quadratic model for UVAG. This model represents a strategic shift from reactive, trial-and-error process development to a proactive, science-based approach. For manufacturing engineers, it is a tool that de-risks process development, enhances technology transfer from the laboratory to production, and provides a quantitative foundation for process capability analysis. By providing a clear roadmap to achieving a desired surface finish, the model facilitates enhanced quality control, reduces scrap rates, and improves overall process efficiency.

The contributions of this study are significant, yet they exist within a defined scope, making it essential to acknowledge the research's inherent limitations.

5.3 Acknowledgment of Limitations

To provide context for the findings, it is essential to acknowledge the boundaries of this investigation and the factors that may have influenced the results. Acknowledging these limitations not only clarifies the scope of the current findings but also establishes a clear foundation for future research. The primary limitations of this study are as follows:

1. **Residual Magnetism in MFAG:** The application of a magnetic field creates the potential for residual magnetism in both the workpiece and the grinding wheel. As noted by Khan et al. (2013), this residual field could act as a confounding variable by promoting chip adhesion even after the primary magnetic source is removed, potentially affecting the accuracy of subsequent surface roughness measurements.
2. **Progressive Tool Wear:** The gradual wear of abrasive grains on the grinding wheel was an uncontrolled variable. Over the course of multiple experiments, this progressive degradation could have altered the wheel's cutting efficiency, thereby introducing variability into the surface roughness results that is not accounted for by the primary process parameters.
3. **Unmeasured Thermal Effects:** While grinding inherently generates significant heat at the tool-workpiece interface, the resulting residual stresses and microstructural changes in the workpiece surface were not directly measured. These thermal effects could have influenced the final surface integrity and represent an unquantified variable in the experimental outcomes.

These acknowledged limitations directly inform and motivate the subsequent recommendations for future avenues of inquiry.

5.4 Future Recommendations

Based on the findings and limitations of this study, this section proposes specific, actionable directions for subsequent research. These recommendations are designed to build upon the current work, address its limitations, and further advance the field of grinding process monitoring and control.

- **Expanded Material and Process Investigation:** Future work should extend the experimental framework to a wider range of materials. A particular focus should be placed on hard and brittle materials, for which UVAG is traditionally considered highly effective. This would test the generalizability of the current findings and broaden the applicability of the developed models.
- **In-Depth Analysis of Resonance Phenomena:** The superior performance observed at 40 kHz in the UVAG experiments warrants a focused investigation. It is recommended that future research employ formal modal analysis, as discussed in the literature review, to identify the natural frequencies of the machine-tool-workpiece system. Confirming that 40 kHz corresponds to a natural frequency would validate the resonance hypothesis and provide a deeper understanding of the underlying physics.
- **Multi-Sensor Data Fusion for Holistic Monitoring:** To fully address the original research problem's call for a "holistic view," future research should integrate the current vibration-based approach with other sensor technologies. As identified in the literature, this could include acoustic emission sensors, thermal imaging cameras, or micromagnetic techniques like Barkhausen noise analysis (Ahrens et al., 2014; Jedamski et al., 2020). Fusing data from multiple sources would enable the development of a more comprehensive, multi-factor coupled model of the grinding process.
- **Development of a Real-Time Control System:** The next logical step is to leverage the predictive UVAG model developed in this thesis as the foundation for a real-time, in-process control system. This would involve integrating the model into a control loop that could autonomously adjust process parameters (e.g., workpiece RPM) to maintain optimal surface roughness, aligning with the future trends toward intelligent manufacturing and active process control.

Pursuing these research directions will help build a more complete and robust understanding of advanced grinding dynamics, paving the way for the next generation of manufacturing technologies.

5.5 Concluding Remarks

This thesis addressed the critical industrial problem of process anomaly control in precision grinding. Beginning with the identification of a gap in existing monitoring techniques, this work systematically investigated the influence of advanced assistance methods—Magnetic Field-Assisted Grinding and Ultrasonic Vibration-Assisted Grinding—on process outcomes. The research yielded novel insights into the complex, frequency-specific dynamics of UVAG and the competing physical phenomena governing MFAG. The culmination of this effort was the development and validation of a predictive mathematical model for the UVAG process, providing a practical tool for industrial process optimization. Ultimately, this work contributes to the foundational shift from process monitoring to embedded process intelligence, establishing a methodology where manufacturing systems can autonomously predict and optimize for quality, thereby advancing the core principles of intelligent, resilient, and sustainable industrial practice.

References

Ahrens, M., Fischer, R., Dagen, M., Denkena, B., & Ortmaier, T. (2014, June). Active chatter damping in plunge grinding using magnetic actuators. In *International Manufacturing Science and Engineering Conference* (Vol. 45806, p. V001T04A037). American Society of Mechanical Engineers. https://doi.org/10.1115/MSEC2014-4111

Altintas, Y., & Weck, M. (2004). Chatter stability of metal cutting and grinding. *CIRP annals*, *53*(2), 619-642. https://doi.org/10.1016/S0007-8506(07)60032-8

Bo, Q., Jiao, A., Zhang, J., Li, H., & Bi, S. (2024). Experimental study on sheet grinding based on magnetic abrasive tool driven by variable electromagnetic fields. *The International Journal of Advanced Manufacturing Technology*, *135*(1), 899-913. https://doi.org/10.1007/s00170-024-14551-2

Box, G. E. P., Hunter, J. S., & Hunter, W. G. (2005). *Statistics for experimenters: Design, innovation, and discovery* (2nd ed.). Wiley.

Brehl, D. A., & Dow, T. A. (2008). Review of vibration-assisted machining. *Precision engineering*, *32*(3), 153-172. https://doi.org/10.1016/j.precisioneng.2007.08.003

Cui, X., Zhang, C. Z., Zhang, Y. B., Zhang, Z. C., Liang, X. L., Liu, M. Z., ... & Li, C. H. (2025). Magnetic field distribution mechanism and grindability in magnetic traction nano-lubricant grinding of Ti-6Al-4V. *Advances in Manufacturing*, 1-28. https://doi.org/10.1007/s40436-025-00548-x

Das, S., Chinnaiyan, P., Jayaseelan, J., Paulchamy, J., Batako, A., & Pazhani, A. (2024). An Experimental Investigation into the Enhancement of Surface Quality of Inconel 718 Through Axial Ultrasonic Vibration-Assisted Grinding in Dry and MQL Environments. *Journal of Manufacturing and Materials Processing*, *8*(6), 255. https://doi.org/10.3390/jmmp8060255

Derringer, G., & Suich, R. (1980). Simultaneous optimization of several response variables. *Journal of quality technology*, *12*(4), 214-219. https://doi.org/10.1080/00224065.1980.11980968

Dong, G., Zhang, H., Zhou, M., & Zhang, Y. (2013). Experimental investigation on ultrasonic vibration-assisted turning of SiCp/Al composites. *Materials and manufacturing processes*, *28*(9), 999-1002. https://doi.org/10.1080/10426914.2012.709338

Ducharne, B., Sebald, G., Petitpré, H., Lberni, H., Wasniewski, E., & Zhang, F. (2023). Magnetic signatures and magnetization mechanisms for grinding burns detection and evaluation. *Sensors*, *23*(10), 4955. https://doi.org/10.3390/s23104955

ElBidweihy, H., Burgy, C. D., Della Torre, E., & Wun-Fogle, M. (2013). Modeling and experimental analysis of magnetostriction in high strength steels. In *EPJ Web of Conferences* (Vol. 40, p. 13005). EDP Sciences. https://doi.org/10.1051/epjconf/20134013005

Gao, Y., Chen, P., Zhang, G., Li, Z., & Yan, R. (2024). Research on grinding force modelling of spherical alumina magnetic abrasive powder. *The International Journal of Advanced Manufacturing Technology*, *131*(3), 1601-1614. https://doi.org/10.1007/s00170-024-13171-0

Han, M., Tang, Y., Ding, W., Zhao, J., Zhao, B., Liu, G., ... & Tang, M. (2023). Study on grinding performance during ultrasonic vibration-assisted grinding ultra-high strength steels. *The International Journal of Advanced Manufacturing Technology*, *128*(7), 3673-3684. https://doi.org/10.1007/s00170-023-12147-w

Hristoforou, E., Ktena, A., Vourna, P., & Argiris, K. (2018). Dependence of magnetic permeability on residual stresses in alloyed steels. *AIP Advances*, *8*(4). https://doi.org/10.1063/1.4994202

Huang, W. T., Cheng, Y. H., Tsai, J. T., & Ho, W. H. (2025). Development of a magnetic field-assisted grinding system and multi-objective optimization of titanium alloy grinding processes. *The International Journal of Advanced Manufacturing Technology*, *139*(7), 3291-3309. https://doi.org/10.1007/s00170-025-16032-6

Hurley, M. E., Bollineni, R. K., Donald, A. M., Flynn, S., Hamlin, J. J., Kesler, M. S., ... & Miller, V. M. (2025). Microstructural Evolution of Steel During Magnetic Field-Assisted Processing. *JOM*, 1-13. https://doi.org/10.1007/s11837-025-07240-2

Inasaki, I., Karpuschewski, B., & Lee, H. S. (2001). Grinding chatter–origin and suppression. *CIRP annals*, *50*(2), 515-534. https://doi.org/10.1016/S0007-8506(07)62992-8

Jedamski, R., Heinzel, J., Rößler, M., Epp, J., Eckebrecht, J., Gentzen, J., ... & Karpuschewski, B. (2020). Potential of magnetic Barkhausen noise analysis for in-process monitoring of surface layer properties of steel components in grinding. *tm-Technisches Messen*, *87*(12), 787-798. https://doi.org/10.1515/teme-2020-0048

Jiang, L., Chang, T., Zhang, G., Chen, Y. S., Liu, X., & Zhang, H. (2023). Effects of machining gap on the surface integrity in CBN spherical magnetic abrasives grinding of ZrO2 ceramic. *The International Journal of Advanced Manufacturing Technology*, *129*(1), 825-835. https://doi.org/10.1007/s00170-023-12343-8

Jiang, L., Zhang, G., Zhang, H., Xia, Y., & Xiang, J. (2024). A Comparative Study of Machining Property in Inconel 718 Superalloy Grinding with Al2O3-and CBN/Fe-Based Spherical Magnetic Abrasives. *Coatings*, *14*(6), 686. https://doi.org/10.3390/coatings14060686

Jin, J., Mao, J., Wang, R., & Cui, M. (2025). Experimental Study on Ultrasonic Vibration-Assisted Grinding of SiCp/Al Composites Grinding. *Micromachines*, *16*(3), 302. https://doi.org/10.3390/mi16030302

Khan, A. A., Ndaliman, M. B., Ali, M. Y., Muath, D., Haazin, A. F., Ibrahim, A., & Mustapa, M. S. (2013, July). The effect of EDM with external magnetic field on surface roughness of stainless steel. In *Int. Conf. Mech. Aut. Aer. Engg*.

Li, H., Chen, T., Bie, W., Chen, F., Suo, Y., & Duan, Z. (2024). Multi-Step Two-Dimensional Ultrasonic-Assisted Grinding of Silicon Carbide: An Experimental Study on Surface Topography and Roughness. *Micromachines*, *15*(7), 915. https://doi.org/10.3390/mi15070915

Li, K. M., Hu, Y. M., Yang, Z. Y., & Chen, M. Y. (2012). Experimental study on vibration-assisted grinding. *Journal of manufacturing science and engineering*, *134*(4), 041009. https://doi.org/10.1115/1.4007102

Liu, C., Zhang, Y., Zhu, L., Li, Q., Shu, X., Qin, S., ... & Shi, W. (2025). A Review of Ultrasonic Vibration-Assisted Grinding for Advanced Materials. *Intelligent and Sustainable Manufacturing*, *2*(1), 10001. https://doi.org/10.70322/ism.2025.10001

Liu, S., Bian, Z., Yu, W., & Maslen, E. (2009). The application of active magnetic bearing spindle on highspeed and precise grinding machine. In *The 11th International Symposium on Magnetic Bearings (ISMB11). Nara*.

Malkin, S., & Guo, C. (2007). Thermal analysis of grinding. *CIRP annals*, *56*(2), 760-782. https://doi.org/10.1016/j.cirp.2007.10.005

Malkin, S., & Guo, C. (2008). *Grinding technology: Theory and applications of machining with abrasives* (2nd ed.). Industrial Press.

Marinescu, I. D., Hitchiner, M. P., Uhlmann, E., & Rowe, W. B. (2016). *Handbook of machining with grinding wheels* (2nd ed.). CRC Press.

Montgomery, D. C. (2017). *Design and analysis of experiments* (9th ed.). John Wiley & Sons.

Myers, R. H., Montgomery, D. C., & Anderson-Cook, C. M. (2016). *Response surface methodology: Process and product optimization using designed experiments* (4th ed.). John Wiley & Sons.

Qingyu, M. E. N. G., Bing, G. U. O., Qingliang, Z. H. A. O., Hao Nan, L. I., Mark, J. J., Barbara, S. L., & Xichun, L. U. O. (2023). Modelling of grinding mechanics: A review. *Chinese Journal of Aeronautics*, *36*(7), 25-39. https://doi.org/10.1016/j.cja.2022.10.006

Qiu, Y., Zhao, B., Cao, Y., Ding, W., Fu, Y., & Pu, C. (2022). On the grinding performance of alumina wheels in ultrasonic vibration–assisted grinding of hardened GCr15 steel. *The International Journal of Advanced Manufacturing Technology*, *120*(3), 1695-1706. https://doi.org/10.1007/s00170-022-08894-x

Santa-Aho, S., Vippola, M., Sorsa, A., Latokartano, J., Lindgren, M., Leiviskä, K., & Lepistö, T. (2012). Development of Barkhausen noise calibration blocks for reliable grinding burn detection. *Journal of Materials Processing Technology*, *212*(2), 408-416. https://doi.org/10.1016/j.jmatprotec.2011.10.003

Tönshoff, H. K., Karpuschewski, B., & Regent, C. (1999). Process monitoring in grinding using micromagnetic techniques. *The International Journal of Advanced Manufacturing Technology*, *15*(10), 694-698. DOI:10.1007/s001700050121

Tsai, H. H., & Hocheng, H. (1998). Investigation of the transient thermal deflection and stresses of the workpiece in surface grinding with the application of a cryogenic magnetic chuck. *Journal of materials processing technology*, *79*(1-3), 177-184. https://doi.org/10.1016/S0924-0136(98)00008-9

Van Oosterhout, G. W., & Klomp, C. J. (1961). On the effect of grinding upon the magnetic properties of magnetite and zinc ferrite. *Applied Scientific Research, Section B*, *9*(4), 288-296. https://doi.org/10.1007/BF02921815

Wang, D., Fan, H., Xu, D., & Zhang, Y. (2022). Research on grinding force of ultrasonic vibration-assisted grinding of C/SiC composite materials. *Applied Sciences*, *12*(20), 10352. https://doi.org/10.3390/app122010352

Wang, X., Ming, C., Zheng, Y., Hou, N., & Wang, M. (2022). Study on grinding nickel-based superalloy GH4169 with ceramic bond CBN wheel controlling abrasive orientation by magnetic field. *The International Journal of Advanced Manufacturing Technology*, *121*(9), 6635-6645. https://doi.org/10.1007/s00170-022-09764-2

Wu, H., Duan, W., Sun, L., Zeng, J., Li, S., Wang, Q., ... & Chen, Y. (2023). Effect of ultrasonic vibration on the machining performance and mechanism of hybrid ultrasonic vibration/plasma oxidation assisted grinding. *Journal of Manufacturing Processes*, *94*, 466-478. https://doi.org/10.1016/j.jmapro.2023.03.067

Xiao, X., Li, G., & Li, Z. (2021). Prediction of the surface roughness in ultrasonic vibration-assisted grinding of dental zirconia ceramics based on a single-diamond grit model. *Micromachines*, *12*(5), 543. https://doi.org/10.3390/mi12050543

Xu, M., Li, H., & Mu, R. (2024). An investigation of magnetic field distribution for assembly of magnets and its effect on alignment of steel fiber in aligned steel fiber-reinforced concrete. *Frontiers in Materials*, *11*, 1351980. https://doi.org/10.3389/fmats.2024.1351980

Yu, K. Q., Jin, T. H., Dong, X. X., & Chen, Y. (2010). Polishing of Small Workpiece with Complicated Surfaces by Electro-magnetic Grinding Method. *Advanced Materials Research*, *135*, 58-63. https://doi.org/10.4028/www.scientific.net/AMR.135.58

Zou, H., Ying, J., Ma, X., Chen, Y., Han, B., & Zhan, J. (2024). Effect of magnetic needle magnetic particle grinding process on the performance of metal aluminum plates. *Surface Science and Technology*, *2*(1), 17. https://doi.org/10.1007/s44251-024-00046-5

Zou, Y. H., & Shinmura, T. (2002). Development of magnetic field assisted machining process using magnetic machining jig. *Trans. Japan Soc. Mech. Eng. Ser. C*, *68*(669), 1575-1581. https://doi.org/10.1299/kikaic.68.1575